Electron Microscopy I
Lecture 9

TT.Prof. Dr. Yolita M. Eggeler

Laboratory for electron microscopy,
CFN building, 2nd floor, room 215
yolita.eggeler@kit.edu
Phone 608-43724

Contents

Laboratory for Electron Microscopy

Electron microscopy I

4.4 Contrasts in crystalline samples with lattice defects

The two special cases of **dislocation**: **step dislocation ⊥ ; screw dislocation ||**

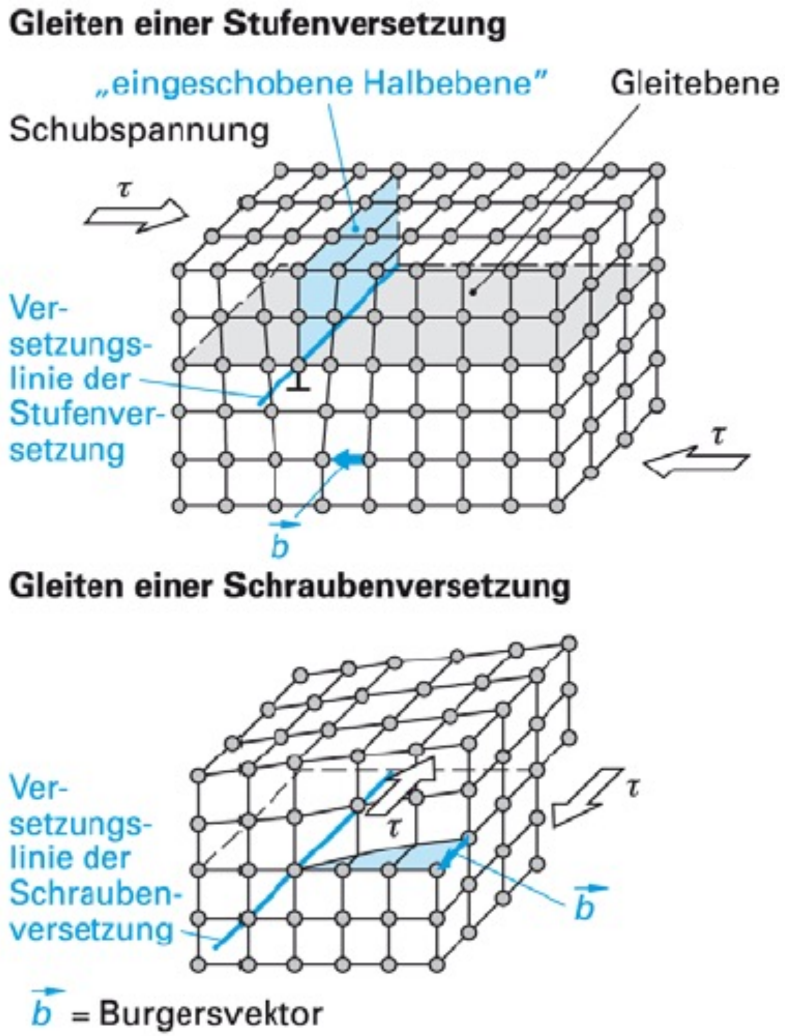

Many dislocations have a mixed character with screw and step components.

Calculation of the scattering amplitude F in crystals with defects

- Defect characterization: Replace all vectors $\vec{r}_{pi}$ with $\vec{r}_{pi} + \vec{R}$ for $\overrightarrow{|R|}$ << lattice plane spacing.
- $\vec{R}$ indicates the displacement of an atom from its regular lattice position.
- Structure factor F_s in good approximation unaffected

$\longrightarrow$ Displacement vector $\vec{R}$ only affects lattice amplitude

$$F = F_S \sum_{\text{All Atoms in column}} \exp\left(2\pi i[\vec{g}+\vec{s}]\left[\vec{r}_{pi}+\vec{R}\right]\right)$$

$$F = F_S \int_0^t \exp\left(2\pi i\left[\vec{g}+\vec{s}\right]\left[\vec{r}+\vec{R}\right]\right) dz$$

$\vec{g}\cdot\vec{r} = integer \longrightarrow \exp(2\pi i \vec{g}\vec{r}) = 1$ and $\vec{s}\vec{R} << \vec{g}\vec{R}$

$$\boxed{F = F_S \int_0^t \exp\left(2\pi i\left[z s_z + \vec{R}\vec{g}\right]\right) dz}$$

Special case: $\vec{g}\cdot\vec{R} = 0$ Defect shows no contrast if $\vec{g} \perp \vec{R}$

4.4 Contrasts in crystalline samples with lattice defects

Two-beam cases for differently reciprocal grid vectors

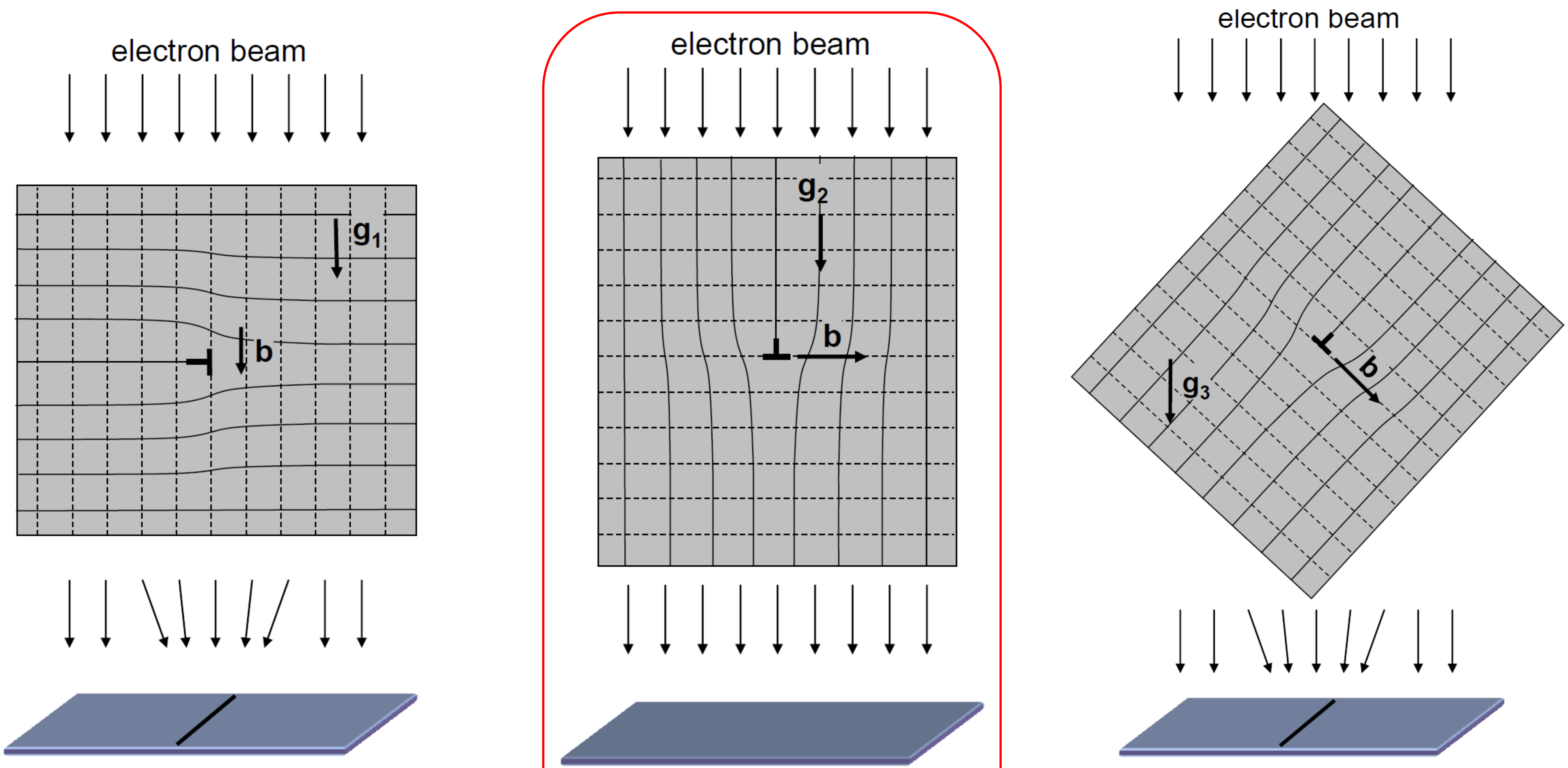

$g_1 \cdot b \neq 0$

$g_2 \cdot b = 0$

Special case: $\vec{g} \cdot b = 0$
Displacement shows no contrast if $\vec{g} \perp \vec{b}$

$g_3 \cdot b \neq 0$

4.4 Contrasts in crystalline samples with lattice defects

Laboratory for Electron Microscopy

Bright field image with s=0

"weak beam" dark field (WBDF) image with s>>0

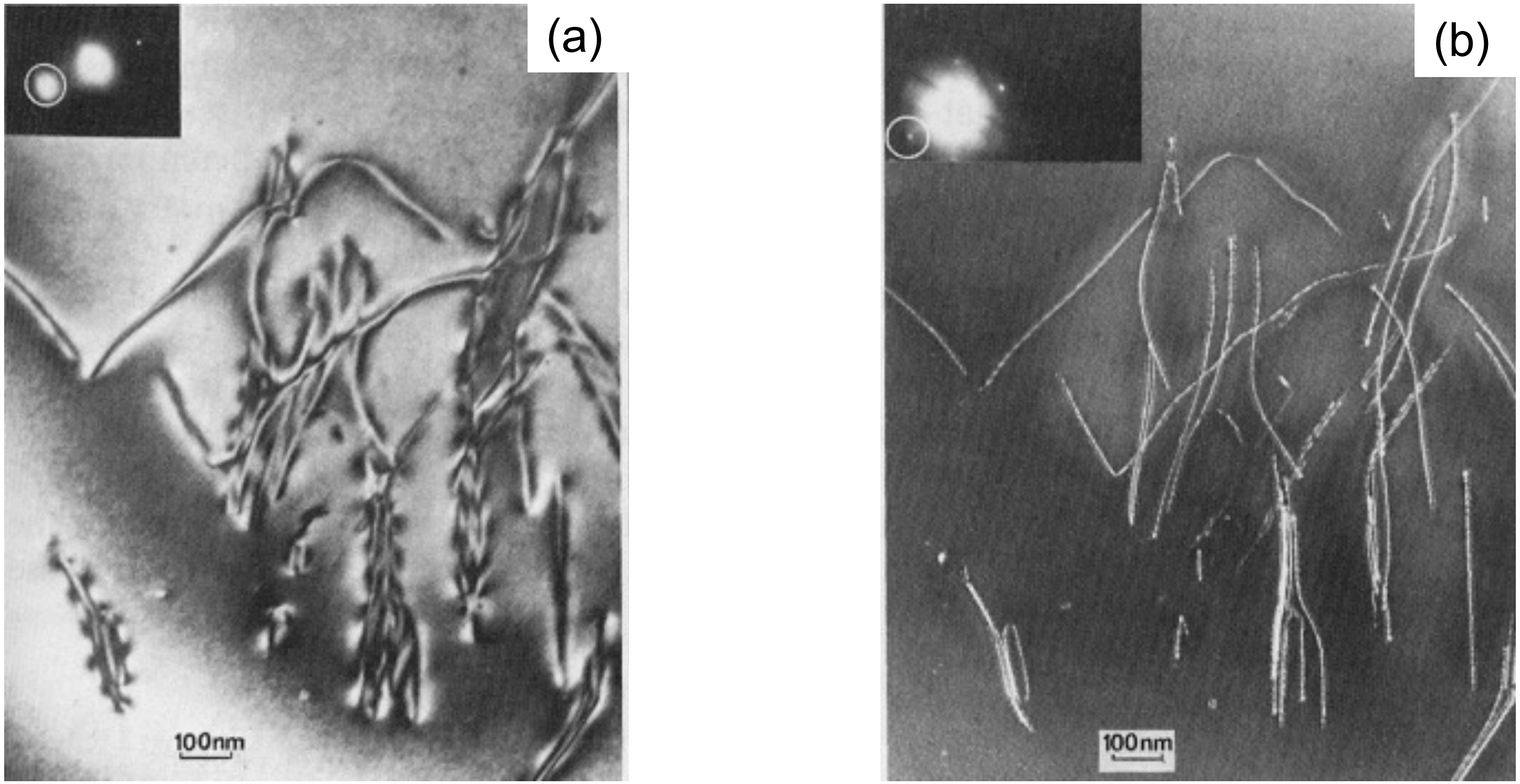

L. Reimer, "Transmission Electron Microscopy", Fig. 8.29

Dark-field TEM images of dislocations in deformed Si with (a) strongly excited $(\bar{2}20)$–reflex. (b) $(\bar{2}20)$ weak-beam dark-field imaging.

Displacement analysis

- Application of the $\vec{g} \cdot \vec{b} = 0$ criterion with two extinctions for $\vec{g}_1$ and $\vec{g}_2$ to determine the direction of $\vec{b} = \vec{g}_1 \times \vec{g}_2$
  (determination of the length more complex, see e.g. Morniroli et al., Phil. Mag. 86, 4883 (2006))

- Complete/unambiguous extinction only if the edge component of the dislocation $\vec{b}_e$ and the line direction $\vec{u}$ are also perpendicular to $\vec{g}$, as the dislocation has a complex displacement field $\vec{R}$ in reality ($\vec{b}$ must be replaced by $\vec{R}$)

$$\vec{R}_{(r,\varphi)} = \frac{1}{2\pi}\left\{\vec{b}\varphi + \vec{b}_e \frac{\sin 2\varphi}{4(1-\nu)} + \vec{b} \times \vec{u}\left(\frac{1-2\nu}{2(1-\nu)} \ln\frac{r}{r_o} + \frac{\cos 2\varphi}{4(1-\nu)}\right)\right\}$$

- In the case of complex crystal structures and elastically highly anisotropic materials, complete/unambiguous extinction is also often not observed

- Calculation of dislocation contrasts using the displacement field $\vec{R}(r,\varphi)$ with the aid of the column approximation most successful but at the same time more complex

  $\rightarrow$ Simulation of different dislocation configurations and comparison of simulated Image contrasts with experimental images
  (see e.g. M. De Graef, Introduction to conventional transmission electron microscopy, Cambridge University Press)

Simulation of dislocation contrasts (column approximation): "Fine structure" of dislocation contrasts

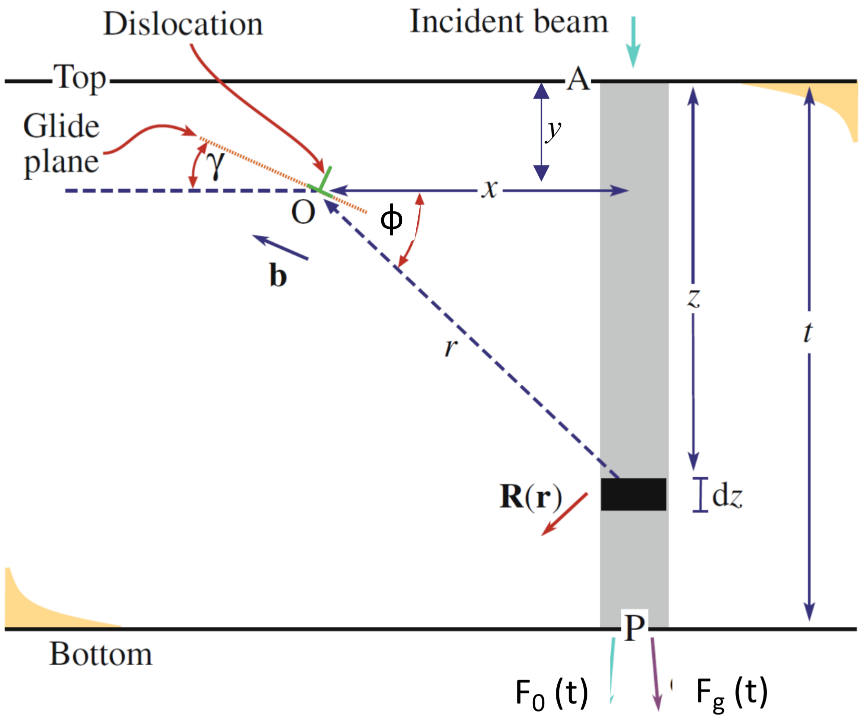

Carter, Williams, Transmission Electron Microscopy, Fig.: 26.2.

- Transfer to depth *y*, *x* = lateral distance of the column from the dislocation core
- Displacement field $\vec{R}$ as a function of the distance *r* from the dislocation kernel and the angle φ for any dislocation (from elasticity theory)
- Calculation of F_g and F_0 by kinematic or dynamic diffraction theory

$$\vec{R}_{(r,\varphi)} = \frac{1}{2\pi}\left\{\vec{b}\,\varphi + \vec{b}_e \frac{\sin 2\varphi}{4(1-\nu)} + \vec{b}\times\vec{u}\left(\frac{1-2\nu}{2(1-\nu)}\ln\frac{r}{r_o} + \frac{\cos 2\varphi}{4(1-\nu)}\right)\right\}$$

r_o : inner cut-off radius of the displacement field $\vec{R}$

ν: Poisson's ratio

$\vec{b}_e$: Edge component of the Burgers vector, φ, *r* : Definition see figure

$\vec{u}$: Unit vector of the dislocation line direction

Simulation of different dislocation configurations and comparison of simulated image contrasts with experimental images.

Bright field image

Experiment **Simulation**

$g_{20.\bar{1}}$

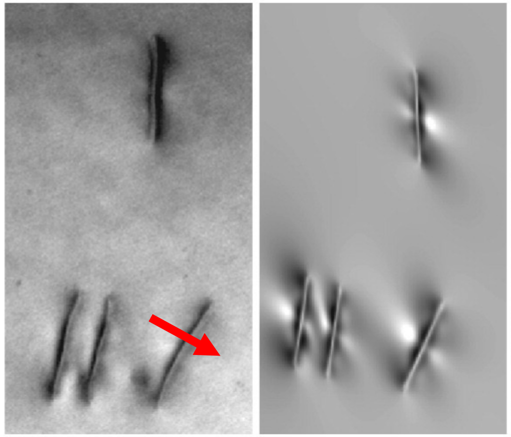

Dark field imaging

Experiment **Simulation**

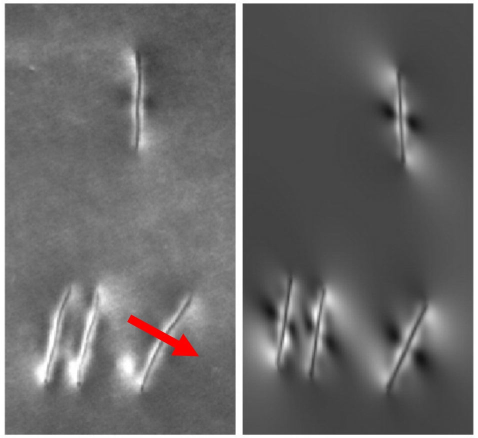

Line profile transverse to the offset (arrow)

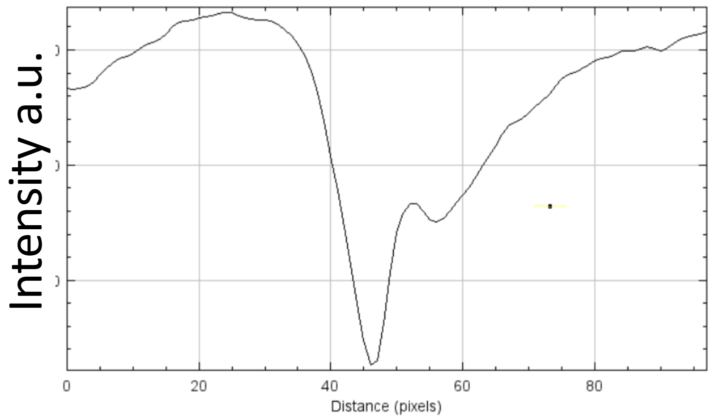

Line profile transverse to the offset (arrow)

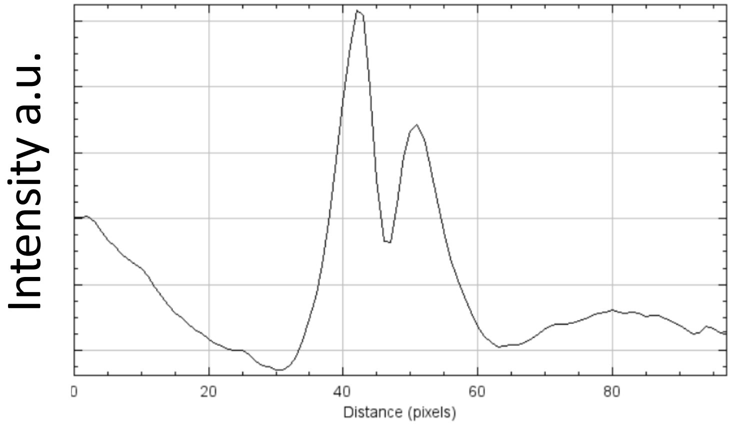

Different contrast lines for different imaging modes of the same offset.

Simulation of dislocation contrasts

Calculated intensities for a screw displacement with
Displacement kernel at $x/\xi_g = 0$
with $\vec{g} \cdot \vec{b} = 2$

with a sample thickness $t = 8\ \xi_g$ for
(a) $w = 0$, $s_z = 0$
Curves 1-3 show dislocations at depths y/ξ_g =4, 4.25 and 4.5

(b) $w = 0.3$, $s_z \neq 0$

ξ_g: Extinction length of the object to be simulated used Bragg Reflexes

$$w = s_z \xi_g$$

Solid lines: Brightfield image
Broken lines: Dark field imaging

P. Hirsch, A. Howie, R.B. Nicholson, D.W. Pashley, J. Wheelan, Electron microscopy of thin crystals, p.254

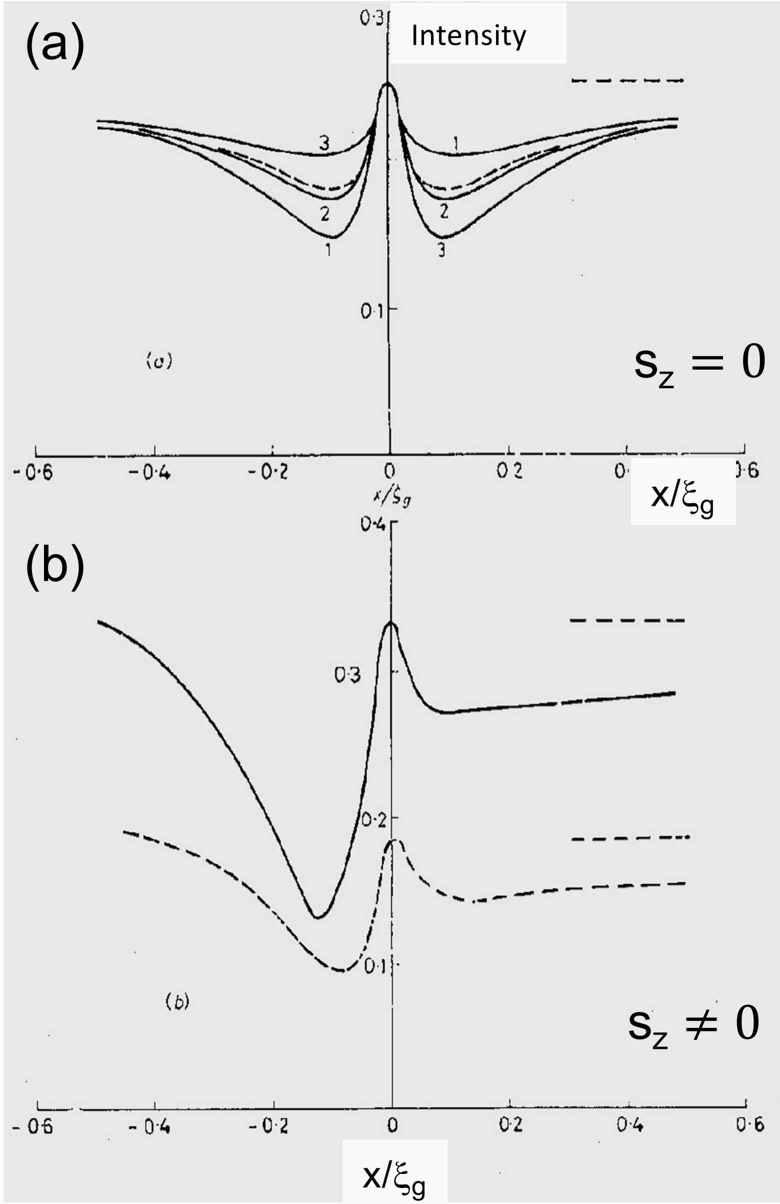

Laboratory for Electron Microscopy

Information from simulation of dislocation contrasts

1. Two contrast lines per offset possible (see simulation on slide 25 and Fig.(a) on slide 9/10 for *w* = 0) for exactly fulfilled Bragg condition (s_z = 0) and $\vec{g} \cdot \vec{b} = 2$

   s_z = 0 unfavorable for the imaging of dislocations (defects in general)

2. In case of deviation from the Bragg case $s_z \neq 0 \rightarrow$ Intensity minimum that is shifted to one side of the dislocation
   (*the sign of s_z determines the direction of the shift in the center of contrast*)

3. Dependence of the contrast width of an offset on extinction length

   the smaller the extinction length, the narrower the contrast (*better separation of the dislocations at small distances*)

   Example: ξ_g = 50 nm $\rightarrow$ typical contrast width ξ_g /5 $\approx$ 10 nm

4. Dislocation contrast depending on the depth of the dislocation in the sample.

Laboratory for Electron Microscopy

Grain boundaries

- Planar defects in polycrystalline samples
- Separation of differently oriented monocrystalline areas (grains)
- "Thickness" of grain boundaries only in the order of a few atomic layers (approx. 1 nm)

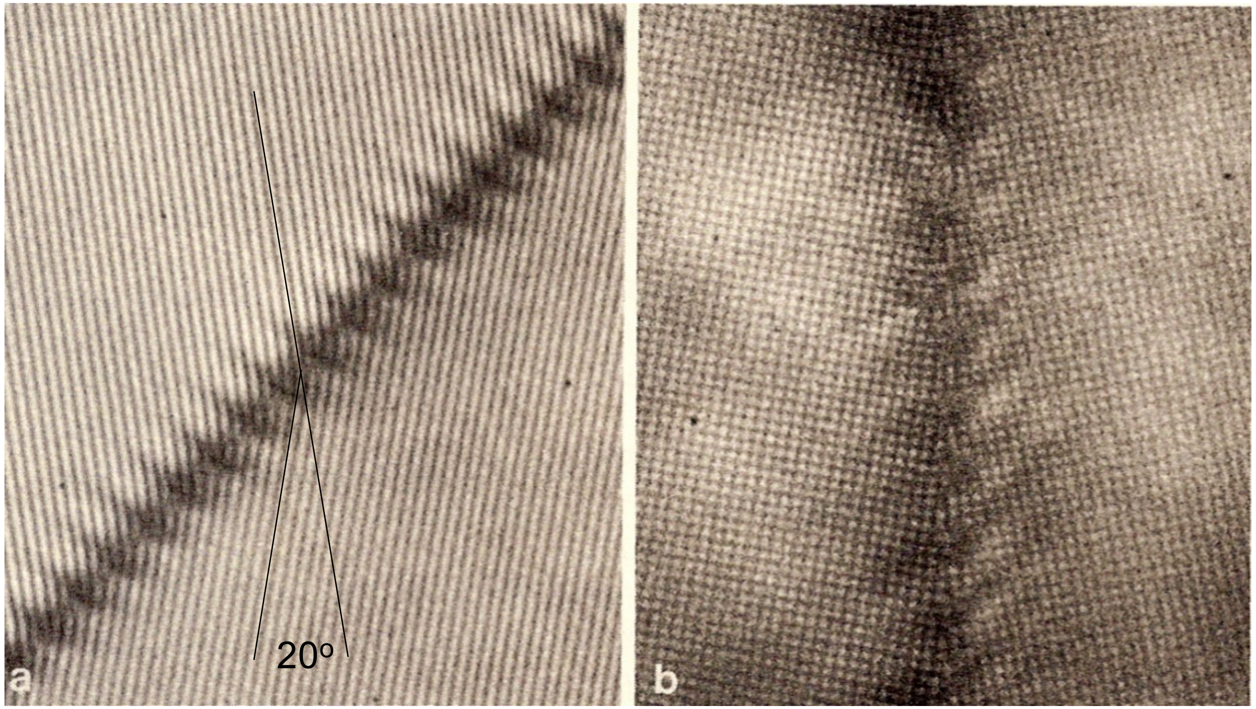

Reimer, "Transmission Electron Microscopy", Fig. 8.11

High resolution TEM images of a 20 degree grain boundary in gold,
a) {200} lattice plane with 0.204 nm lattice plane spacing
b) Crossed lattice planes at a grain boundary in [100] zone axis

Grain boundaries

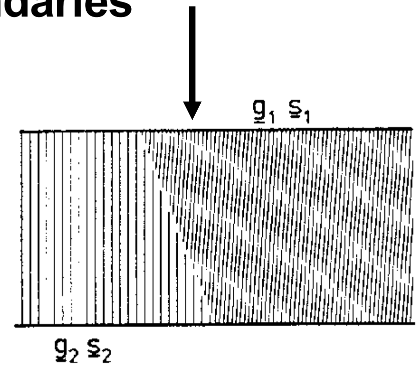

Abb. 4.20 Beugungsbedingungen bei einer Korngrenze. Wenn das obere Korn (rechts) so orientiert ist, daß der Beugungsvektor g mit Abweichung s_1 angeregt ist, dann wird wahrscheinlich ein anderer Vektor (g_2) in dem unteren Korn (links) mit anderem und möglicherweise wesentlich größerem s_2 angeregt.

P.J. Goodhew, J. Humphreys, R. Beanland, Electron Microscopy and Analysis, Fig. 4.23

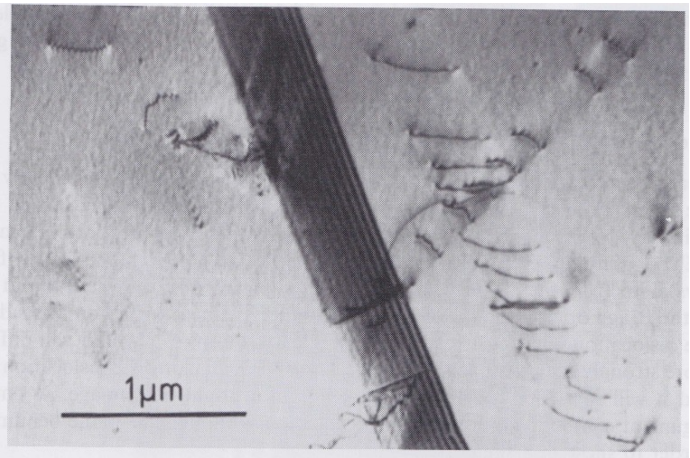

P.J. Goodhew, J. Humphreys, R. Beanland, Electron Microscopy and Analysis, Fig. 4.24

Contrast dependent on excitation of Bragg reflexes in neighboring grains

Different mapping vectors ($\vec{g}_1$, $\vec{g}_2$) and excitation error (s_1, s_2) in neighboring grains

Thickness contours at the grain boundary, if two-beam condition only is present in one grain and in the 2nd grain. No Bragg reflex is strongly stimulated

→ Thickness contours for strongly bending grain

Laboratory for Electron Microscopy

Moiré effect

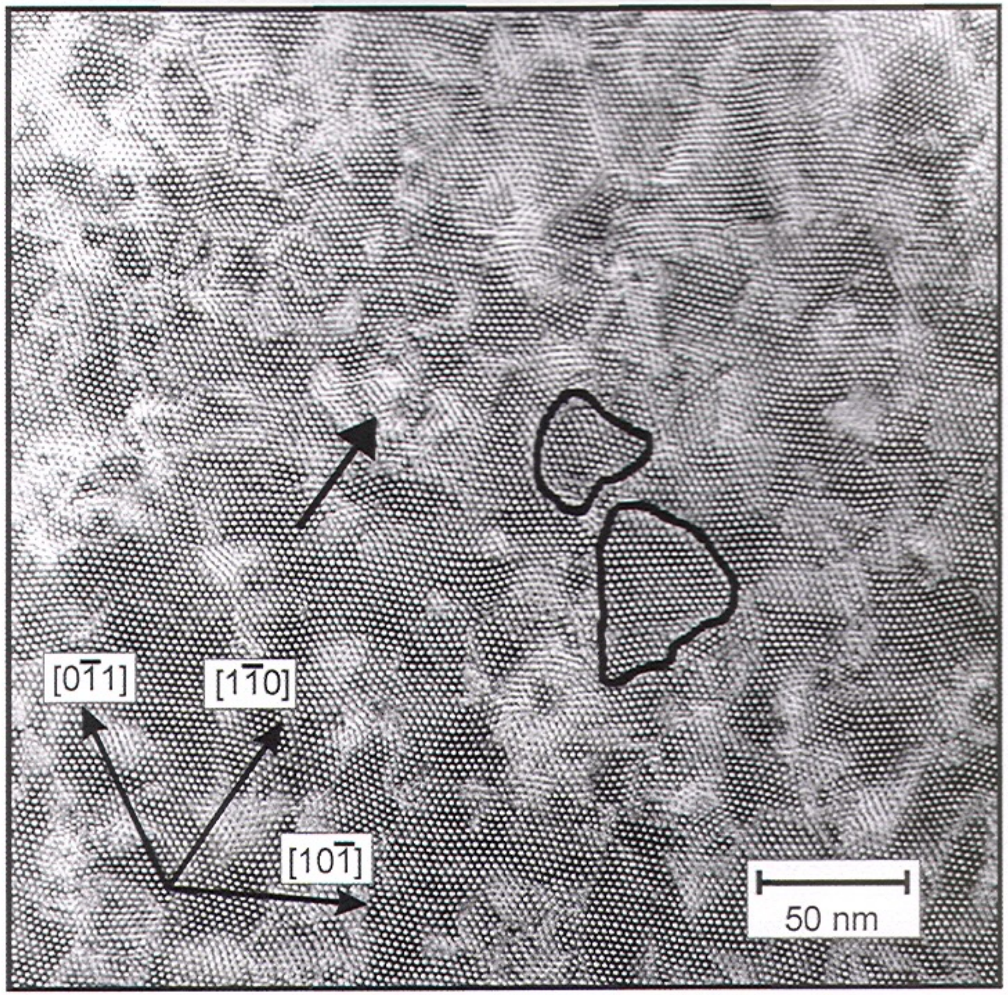

10 nm ZnTe on GaAs(111) substrate
(Diploma thesis A. Wurl, LEM 1998)

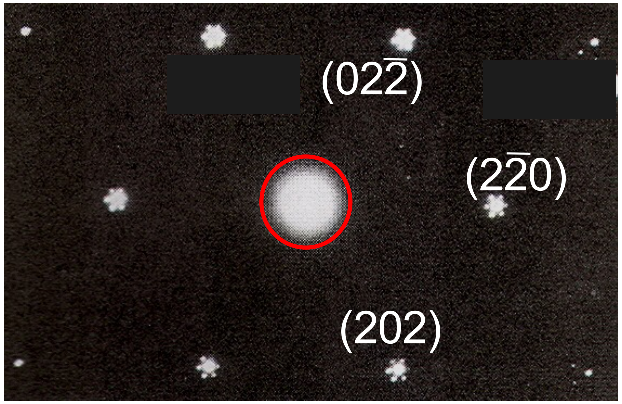

Diffraction image along
[111] Zone axis
with "satellite reflections" around
Bragg Reflexes

GaAs and ZnTe with the same
Crystal structure but under
different lattice constants
a_{GaAs} = 0.564 nm
a_{ZnTe} = 0.6122 nm

Moiré effect with two (or more) strongly diffracting grains in Electron beam direction

Two simple cases:

1. grains with the same orientation and different lattice plane spacings d_1, d_2

2. grains with the same lattice plane spacing d rotated against each other by angle α arranged one above the other in the direction of transmission.

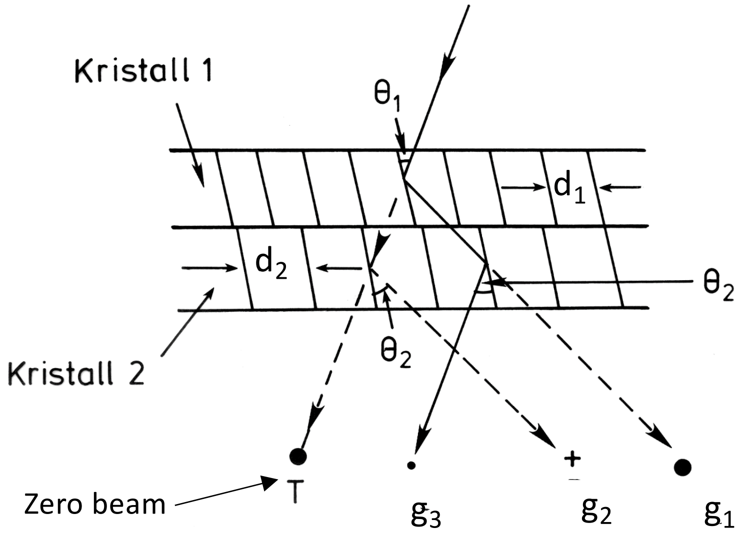

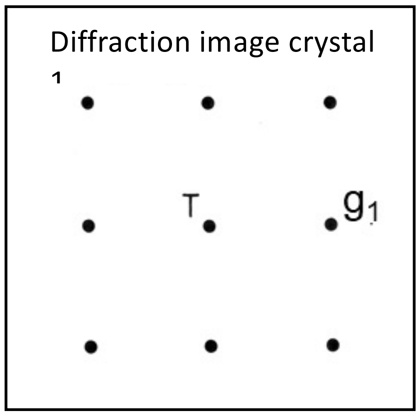

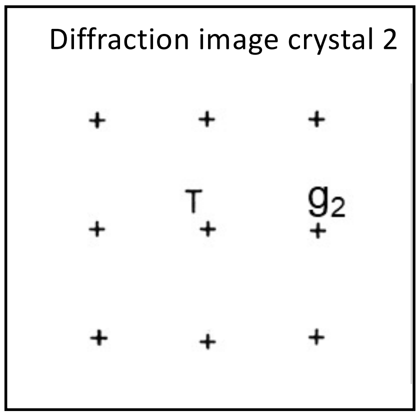

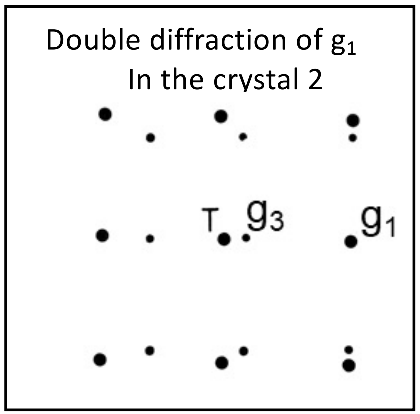

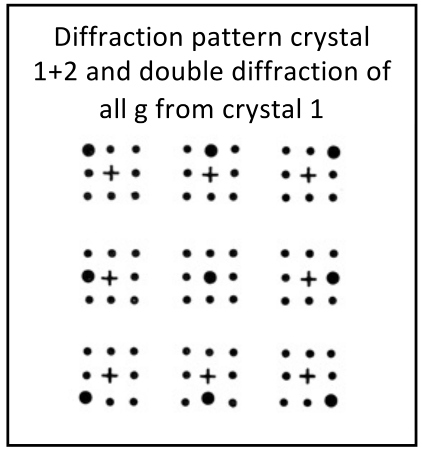

Laboratory for Electron Microscopy

Moiré effect with two (or more) strongly diffracting grains in Electron beam direction

Diffraction pattern (schematic)

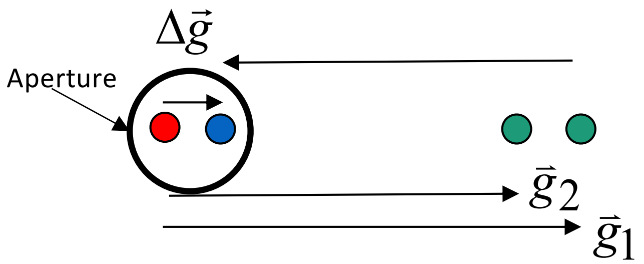

Reflex through double diffraction (blue dot)

Zero beam (undiffracted electrons) (red dot)

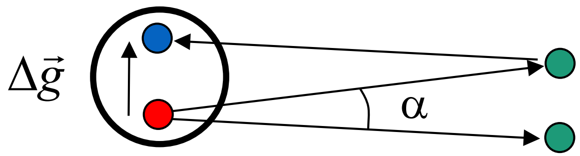

$$\Delta\vec{g} = \vec{g}_1 - \vec{g}_2$$

Determines the distance and orientation of the Interference strip

Translation moiré strips

Case 1
Interference fringe distance D
Parallel to d_1 , d_2

$$\frac{1}{D} = \frac{1}{d_1} - \frac{1}{d_2}$$

Rotary moiré stripes

Case 2
Interference fringe distance D
almost perpendicular to the
for small a

$$\frac{1}{D} = \frac{2\sin\frac{\alpha}{2}}{d}$$

Moiré effect: Optical analog

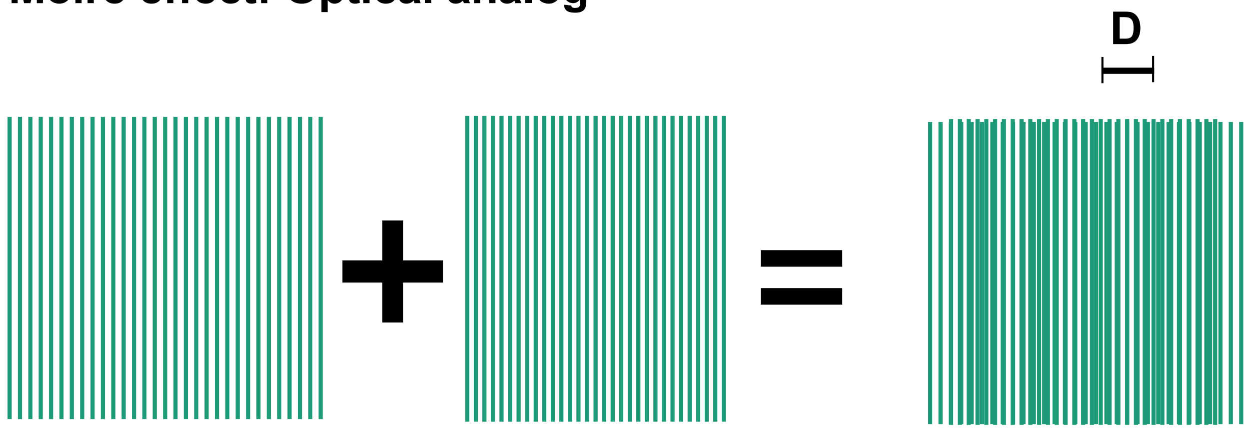

Case 1: Translational moiré strips
Parallel moiré effect

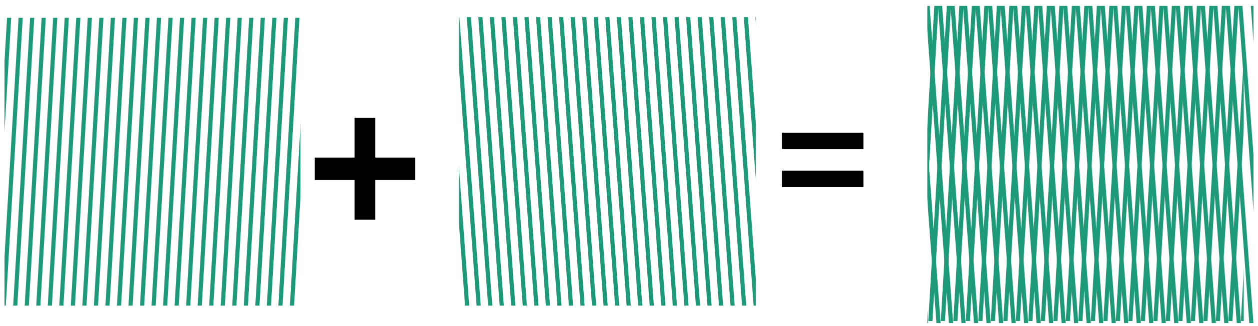

Case 2: Rotation **moiré** effect

D

P. Hirsch et al., "Electron Microscopy of Thin Crystals", Fig. 15.4

Moiré effect: visualization of defects

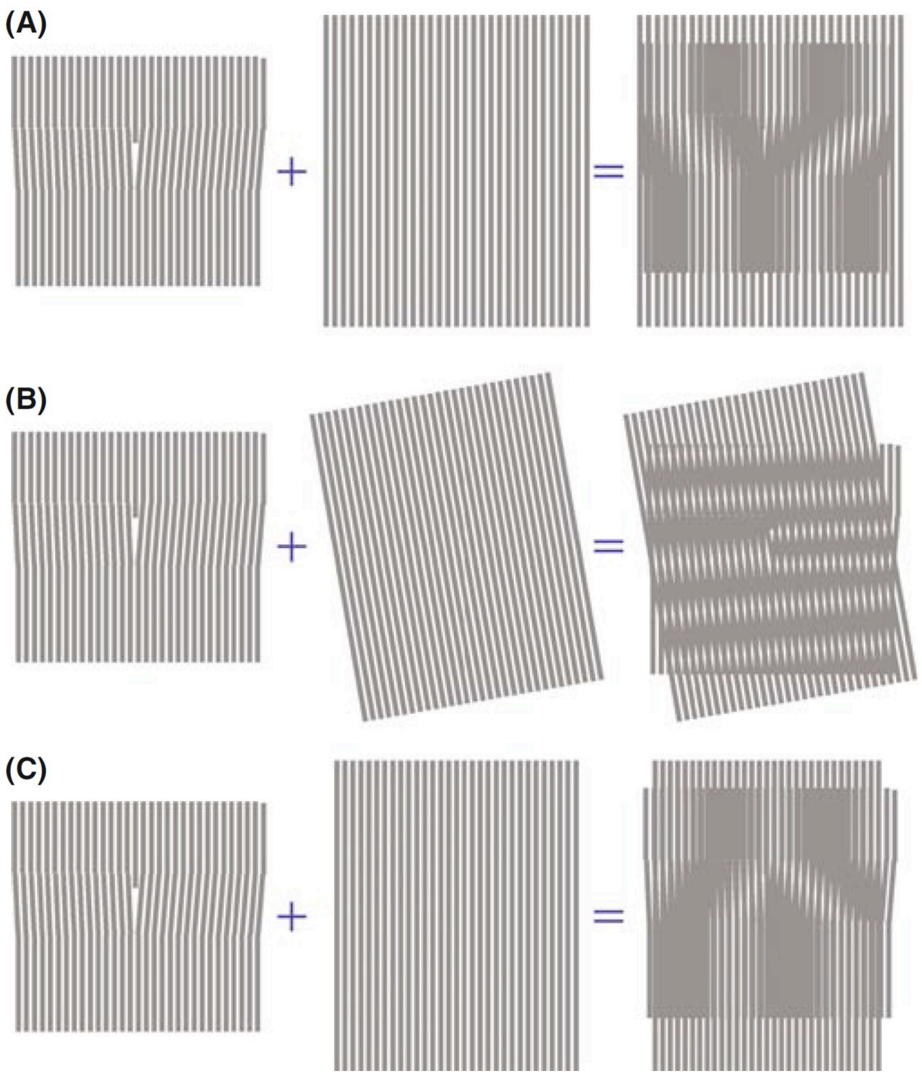

FIGURE 23.11. Schematic diagrams showing why moiré patterns from regions containing dislocations cannot be readily interpreted: (A) a dislocation image formed by interference between a regular lattice and one containing an extra half-plane. (B) In comparison with (A), a small rotation of the lattice of either grain can cause a large rotation of the dislocation fringes. (C) A small spacing change of either lattice can cause the dislocation image to reverse.

D.B. Williams, C.B. Carter,
Transmission Electron Microscopy, Fig. 23.11

Moiré effect

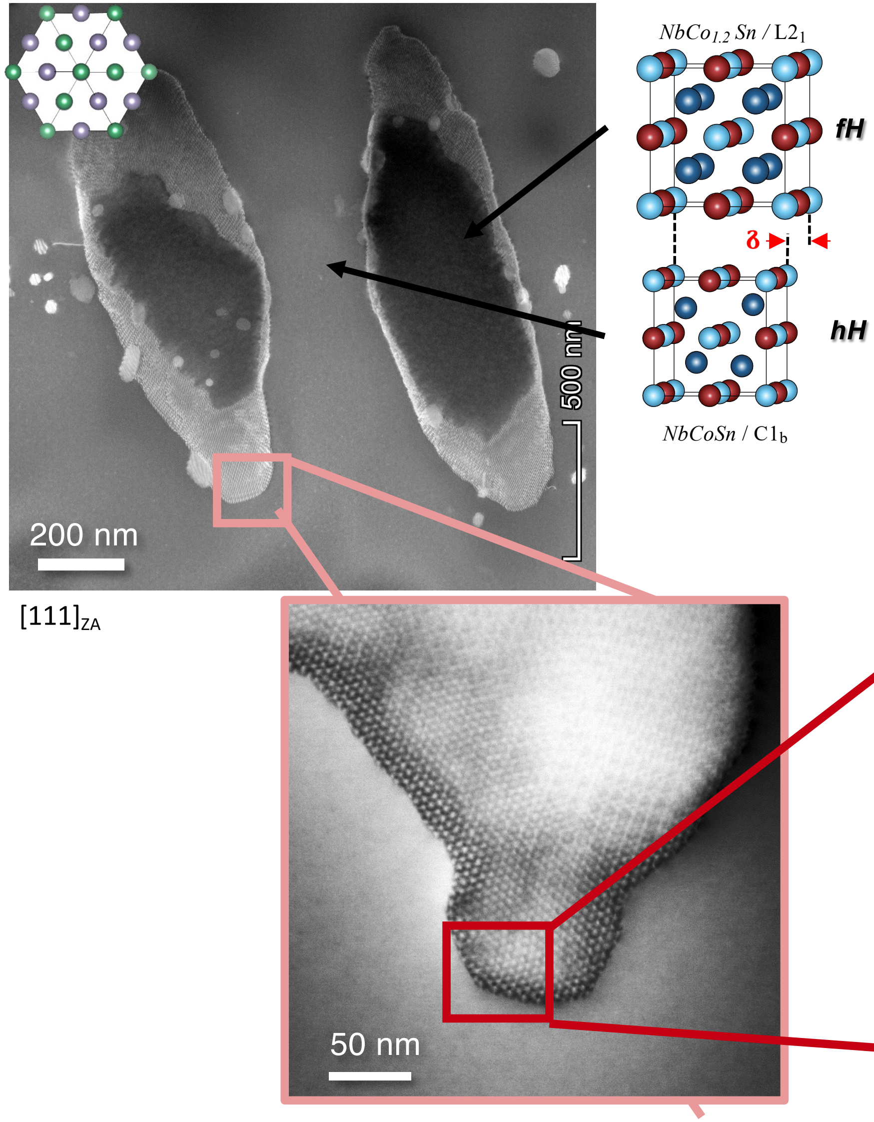

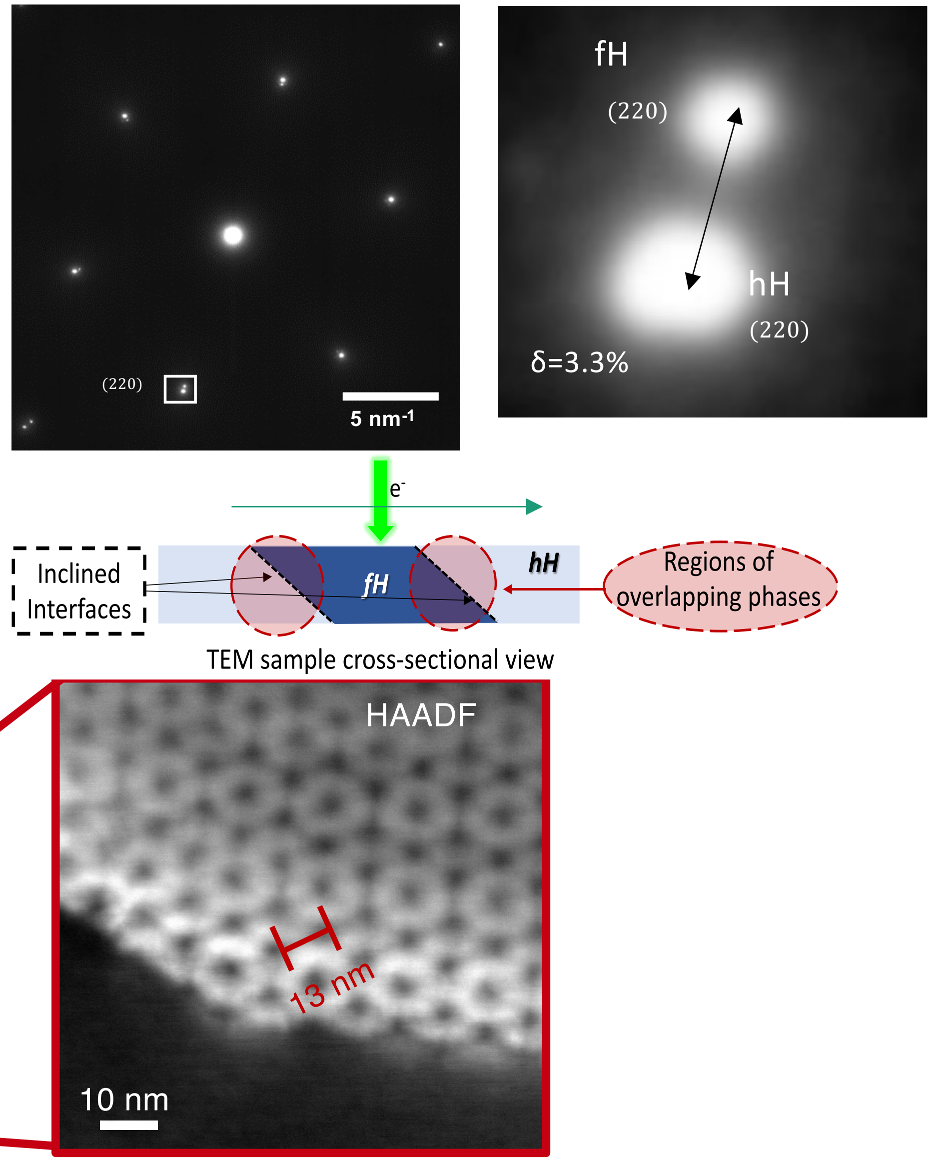

4.4 Contrasts in crystalline samples with lattice defects

Moiré effect: Same orientation of the phases, but lattice plane spacing differs (in the example by 3%).

Full Heusler + Half Heusler

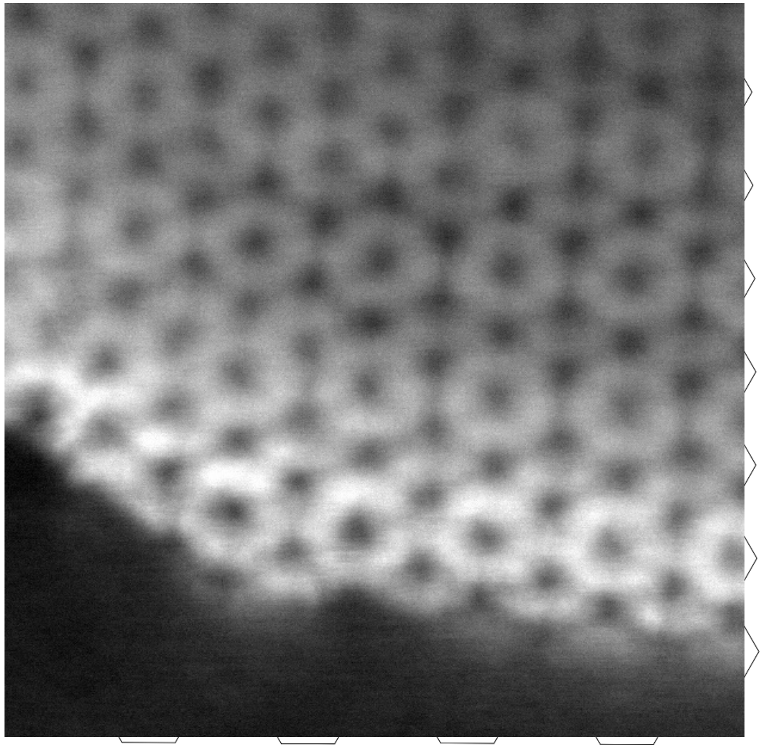

downsizing

Full Heusler + Half Heusler

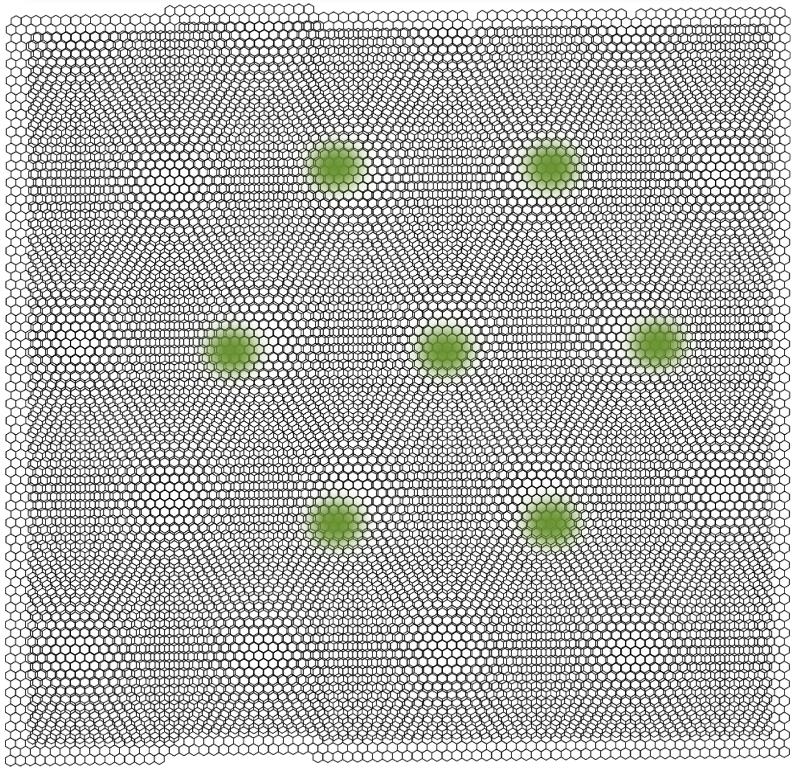

Superposition of both lattices
"Enlarged section"

Superposition of both lattices
"Reduced section"

Translation moiré strips

Laboratory for Electron Microscopy

Three-dimensional defects in multiphase alloys

State diagram of brass (Cu-Zn)

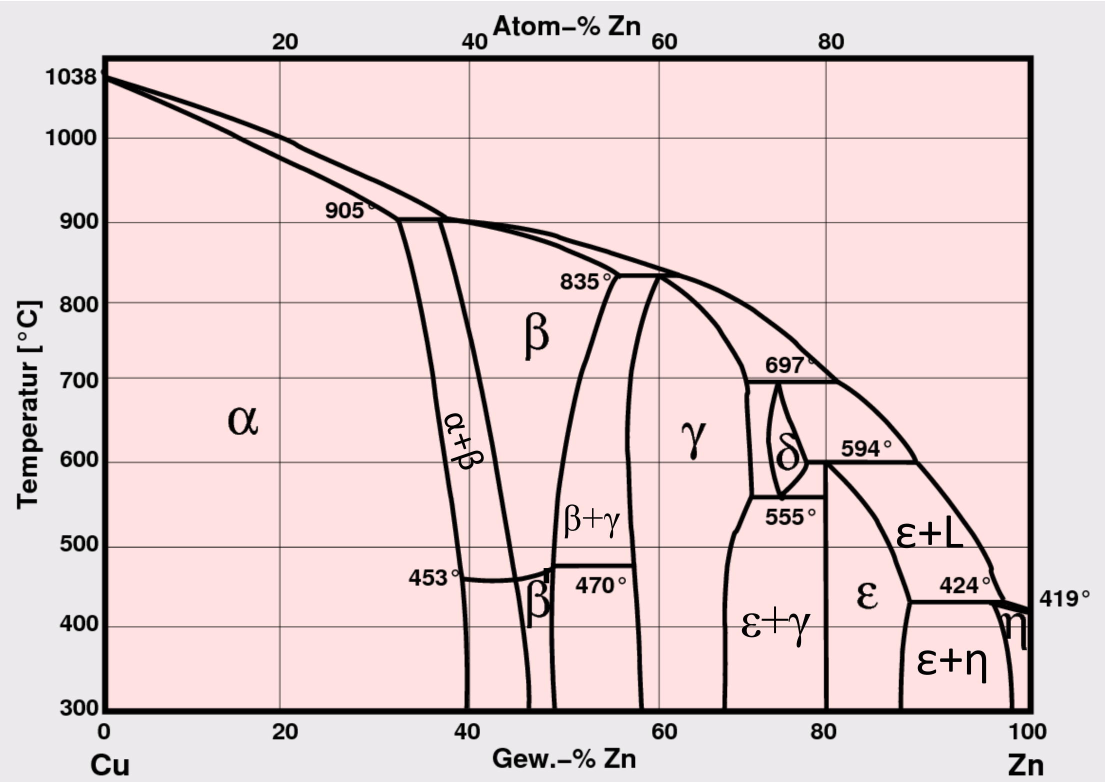

7 thermodynamically stable solid phases with different crystal structures and chemical compositions

α Phase: fcc structure
β phase: bcc structure (β': B2 order)
γ, δ phases: cubic complex with large elementary cells
ε, η Phases: hexagonal with different c/a ratio

Several two-phase areas in which two phases are stable.
→ Precipitates must form in a matrix here

http://ruby.chemie.uni-freiburg.de/Vorlesung/intermetallische_4_4.html

4.5 Analysis of phase mixtures

Description of phases/phase boundaries in multiphase materials by

- Crystal structure of the different phases (possibly also amorphous parts)
- Type and distribution of atoms in the phases (ordered, disordered)
- Shape of the interfaces (straight or curved)
- Volume fractions of the different phases comparable
  or significantly different (small particles embedded in matrix)
- Structure of the interface between the phases characterized by displacementvector

Phase boundaries (red)

Coherent particle:
Lattice constants of particles and matrix are the same.

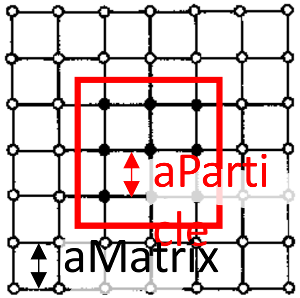

$a_M = a_T$

Coherent particle:
small difference in lattice constants

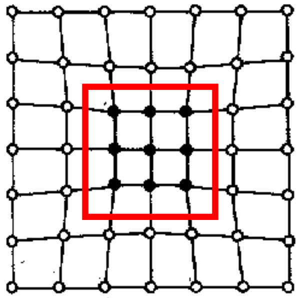

$a_M > a_T$

Partially coherent particle

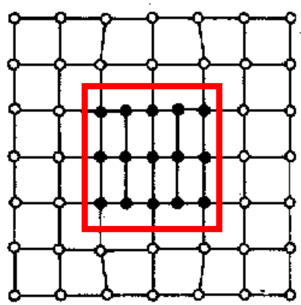

$a_{M\,(horizontal)} = a_{T\,(horizontal)}$

$a_{M\,(vertical)} \neq a_{T\,(vertical)}$

Incoherent particle

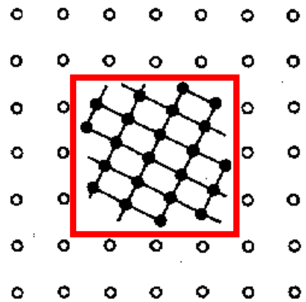

$a_M \neq a_T$

Fuchs, Oppolzer, Rehme, Particle Beam Microanalysis, Fig. 4.47

Laboratory for Electron Microscopy

Contrast of phase boundaries/particles in a matrix

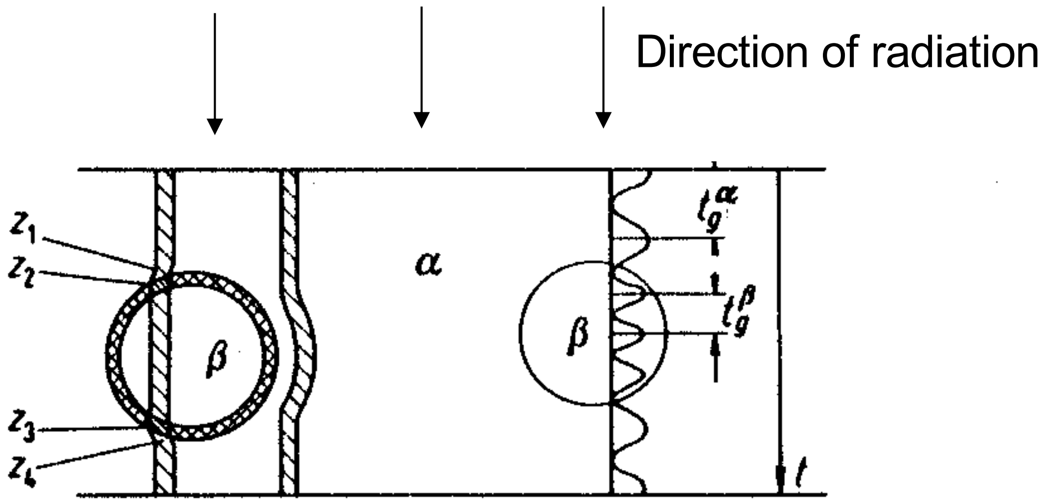

Incoherent particle Uncoherent, coherent particle

Abb. 8.2: Erscheinungen beim Durchgang eines Elektronenstrahls durch Folie (α) mit Teilchen (β). Rechts: kohärentes, unverspanntes Teilchen; es ändert sich nur die Extinktionslänge beim Durchgang durch das Teilchen. Links: allgemeiner Fall, nicht-kohärentes Teilchen, Verspannung des Grundgitter α. z_1 Verzerrung des Grundgitters, z_2 Phasensprung in der Grenzfläche, z_2-z_3 Änderung der Extinktionslänge, z_3 Phasensprung in der Grenzfläche, z_4 Verzerrung der Matrix, t Foliendicke

E. Hornbogen, B. Skrotzki, Materials microscopy, Fig. 8.2

Coherent, spherical particle with the same structure as the matrix
small difference in the lattice constants of matrix and particles

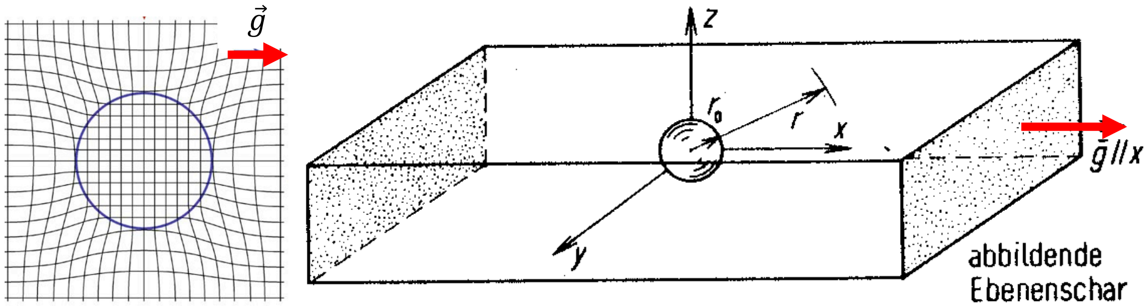

Dominance of the effect of the Tension ε(r) with similar extinction lengths ξ_g of particle and matrix material

Abb. 8.3: Teilchen mit Radius r_0 und kugelsymmetrischem Spannungsfeld. Die Verzerrung $\Delta\vec{r}$ nimmt alle möglichen Richtungen zum abbildenden reziproken Gittervektor $\vec{g}$ ein.

E. Hornbogen, B. Skrotzki, Materials microscopy, Fig. 8.3c

Displacement field with spherical symmetry within the particles with $r < r_0$

$$R(r) = \varepsilon r$$

Outside the particle $r > r_0$

$$R(r) = \frac{\varepsilon r_0^3}{r^2}$$

ε dependent on lattice constant difference and elastic properties of particles and matrix

Coherent, spherical particle in matrix

Coherent particle: Small difference in lattice constants

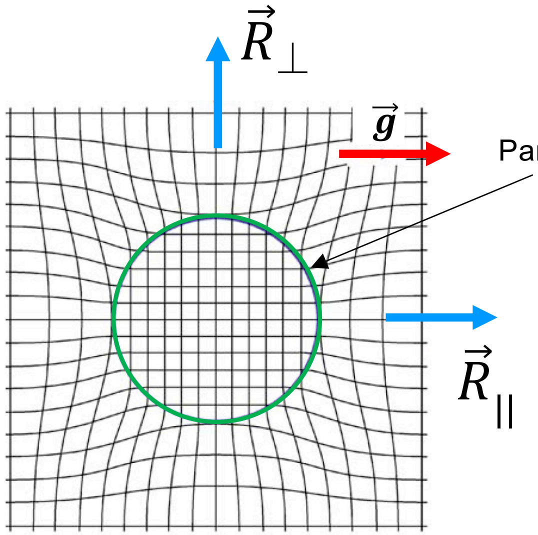

Particles

Simulated intensity contours of the particle (left)

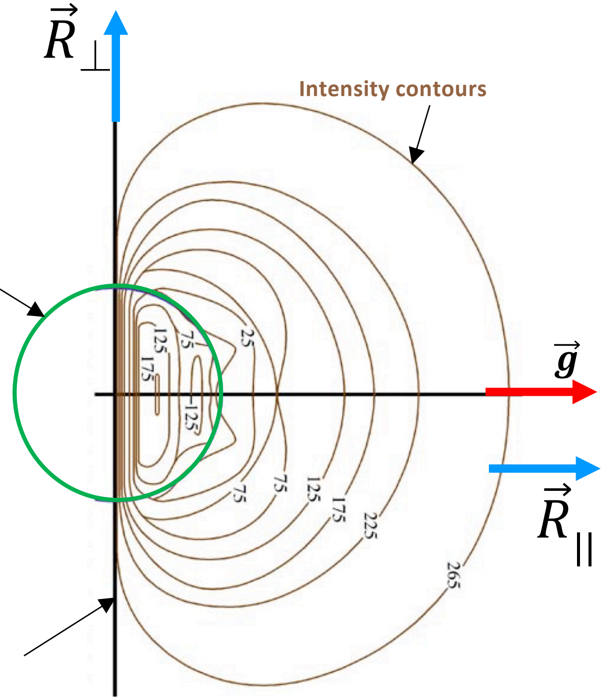

Consider $\vec{g}\cdot\vec{R}$ = 0

Numbers correspond to intensity
Background intensity 272 (bright field image)

Bright field image of coherent cobalt particles with excitation condition g_{220}

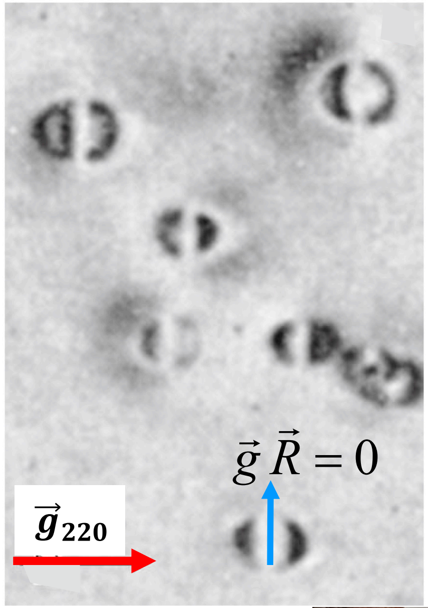

Particle contrast does not reflect the shape and size of the particle, but depends on the depends on the displacement field and imaging vector! "Coffee bean contrast"

Contrast of ordered γ' particles in a Ni-Cr-Ti-Al alloy

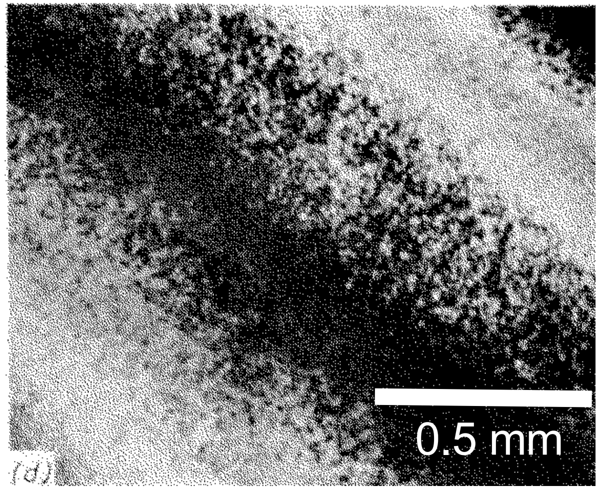

Structure factor contrast (different extinction lengths of particles and matrix) in a bright field image compare illustration of cavities

$$\xi_g = \frac{\pi V_e \cos\theta_B}{\lambda F_{S,g}}$$

P. Hirsch, A. Howie, R. Nicholson, D.W. Pashley, M.J. Whelan, "Electron Microscopy of Thin Crystals", Fig. 14.16 (d,e)

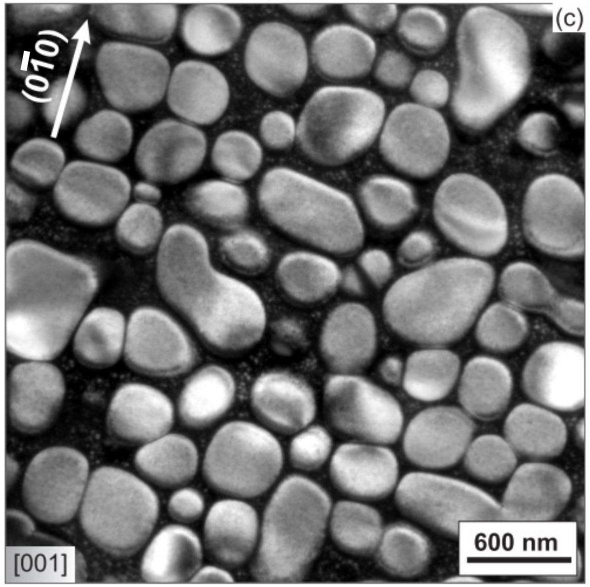

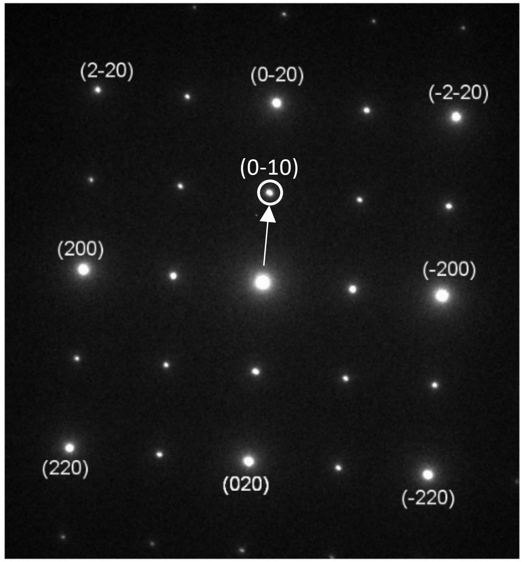

Dark-field imaging with superstructure reflection of particles
with ordered crystal structure

Y.M.Eggeler, Master thesis FAU 2013

4.6 Diffraction patterns / Convergent electron diffraction

Laboratory for Electron Microscopy

Additional literature:
J.C.H. Spence, J.M. Zuo, Electron Microdiffraction, Plenum Press

Information from "conventional" diffraction images

- Lattice parameters and crystal structure by arrangement/symmetry of the Bragg reflexes, e.g. for the identification of phases in combination with chemical information through Energy-dispersive X-ray spectroscopy
- Morphology of small (few nm) particles by shape and expansion of the reflexes
- Setting imaging conditions (imaging vector and excitation error)

Convergent electron diffraction (CBED: Convergent Beam Electron Diffraction)

- Precise grid parameter determination $\Delta a/a=10^{-4}$ with high spatial resolution
- Determination of specimen thickness and absorbance length
- Three-dimensional information about crystal structure
- Precise measurement of acceleration voltages
- Determination of the length of Burgers vectors of dislocations (J. P. Morniroli, J. Microscopy 23,240 (2006))
- Electron density distribution and structure factors

4.6 Diffraction patterns / Convergent electron diffraction

Conventional electron diffraction: parallel illumination / point-like Bragg reflections

SAED

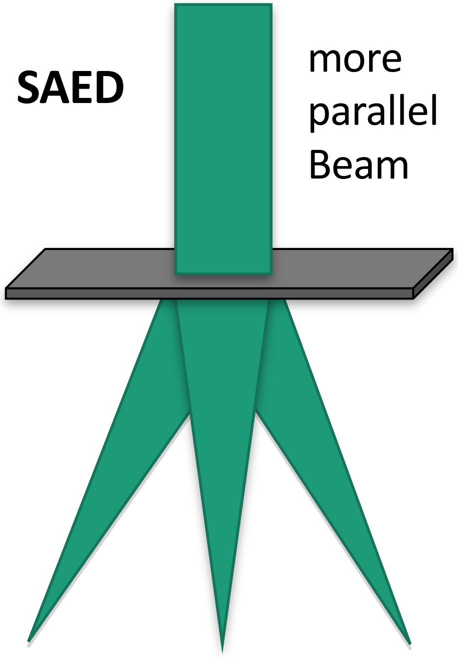

more parallel Beam

Sample

Smallest sample area to be analyzed limited by SAED aperture

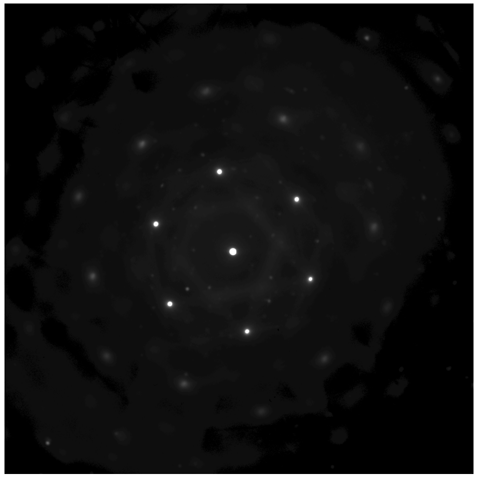

punctiform reflexes

Parallel illumination:
Selection of small sample areas with fine range aperture or in nano-diffraction mode

Convergent electron diffraction: convergent illumination / disk-shaped extended reflections

CBED

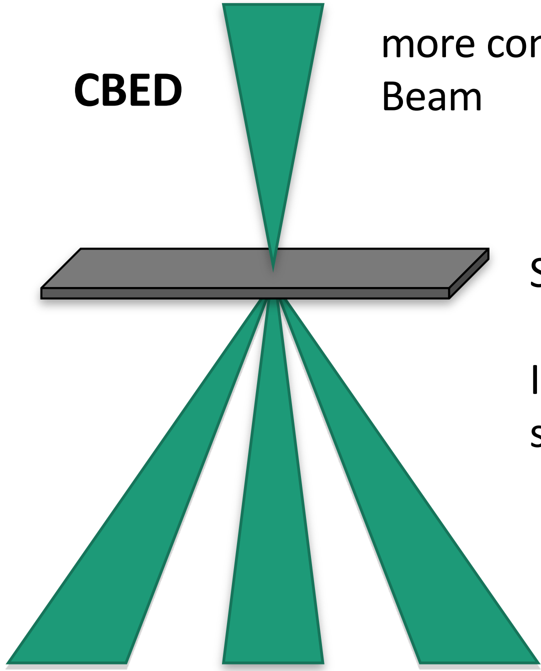

more convergent Beam

Sample

Investigation of very small sample volumes

disc-shaped reflexes

Kikuchi bands easily recognizable

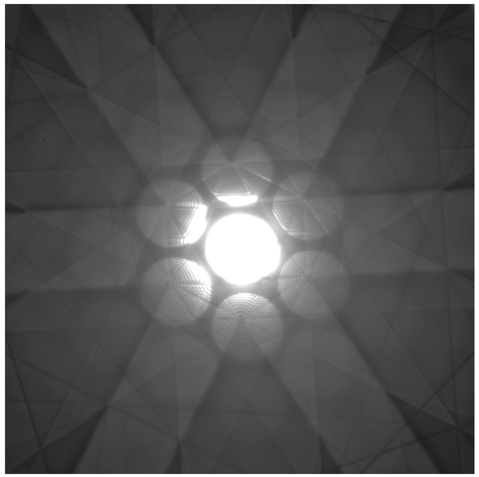

Convergent illumination:
Selection of small sample areas by focusing the electron beam on Small diameter

4.6 Diffraction patterns / Convergent electron diffraction

Laboratory for Electron Microscopy

Ewald construction

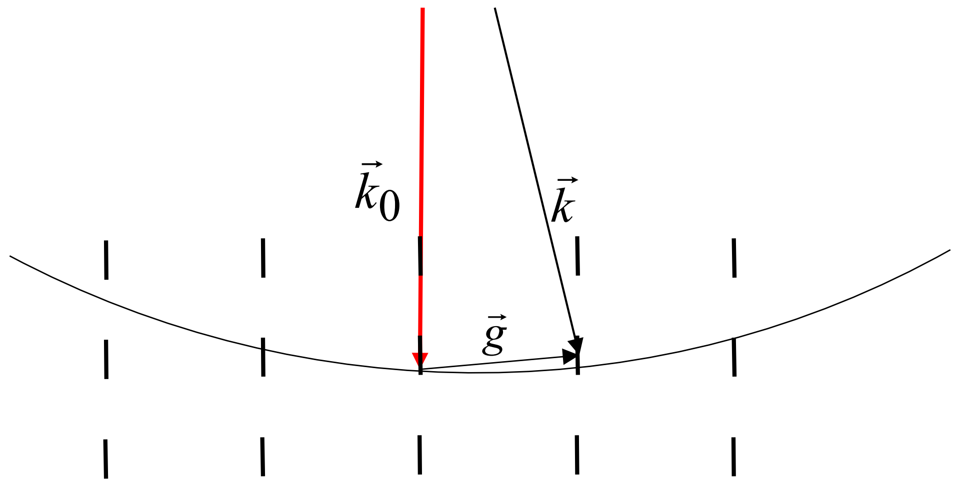

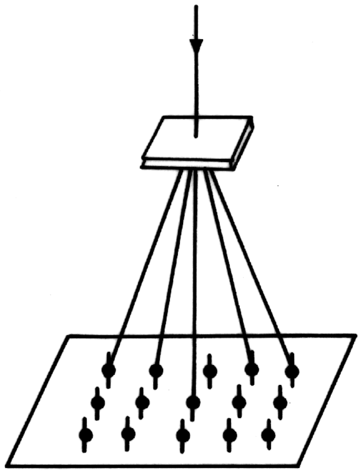

Visualization of $\vec{k} - \vec{k}_0 = \vec{g} + \vec{s}$

Thin sample in the electron beam direction:
⟶ reciprocal lattice *rods* instead of reciprocal lattice points

Surface-like defects generate extended reflections in 2 dimensions,
nanoscale particles in 3 dimensions extended reflexes (Lecture 6 Slide 12-14)

4.6 Diffraction patterns / Convergent electron diffraction

Laboratory for Electron Microscopy

Kikuchi lines

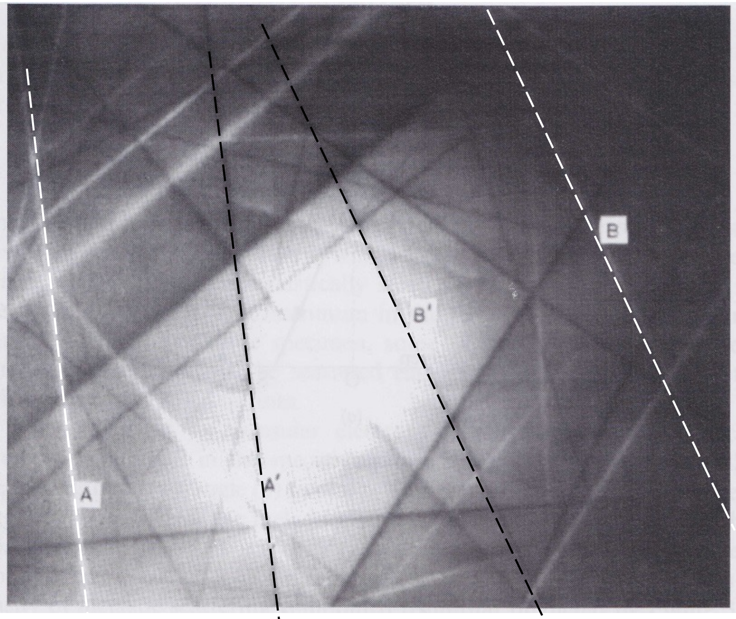

P.J. Goodhew, J. Humphreys, R. Beanland, Electron Microscopy and Analysis, Fig. 3.18

With increasing sample thickness:
Pairs of parallel light and dark lines → Kikuchi lines created by inelastic scattering processes and subsequent elastic (Bragg) diffraction arise

Inelastic Scattering process with *low* Energy loss

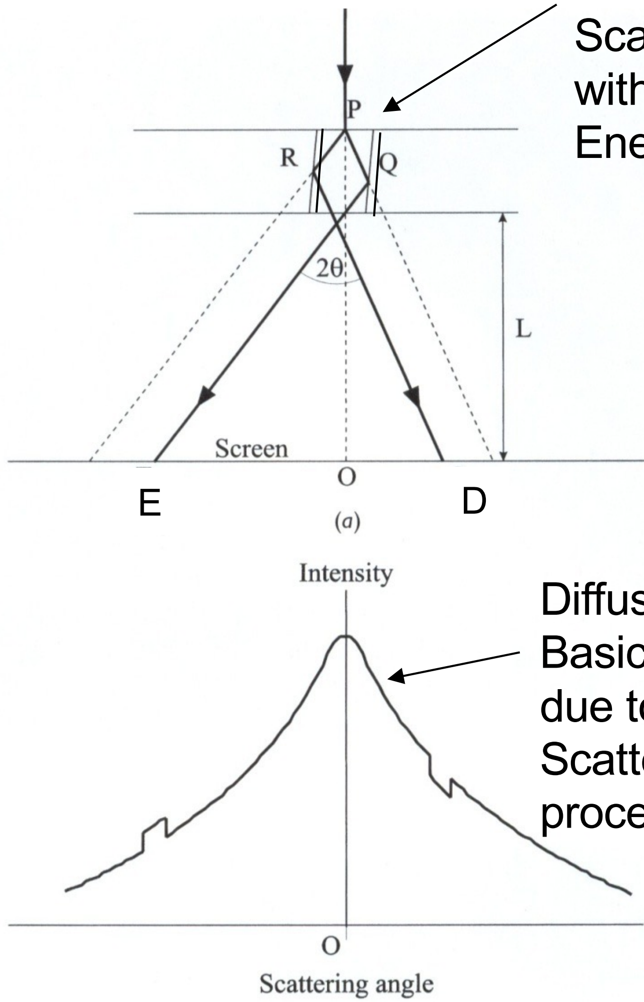

Diffraction image

Diffuse background Basic intensity due to inelastic Scattering processes

P.J. Goodhew, J. Humphreys, R. Beanland, Electron Microscopy and Analysis, Fig. 3.17

Laboratory for Electron Microscopy

Kikuchi lines

Two-stage formation mechanism

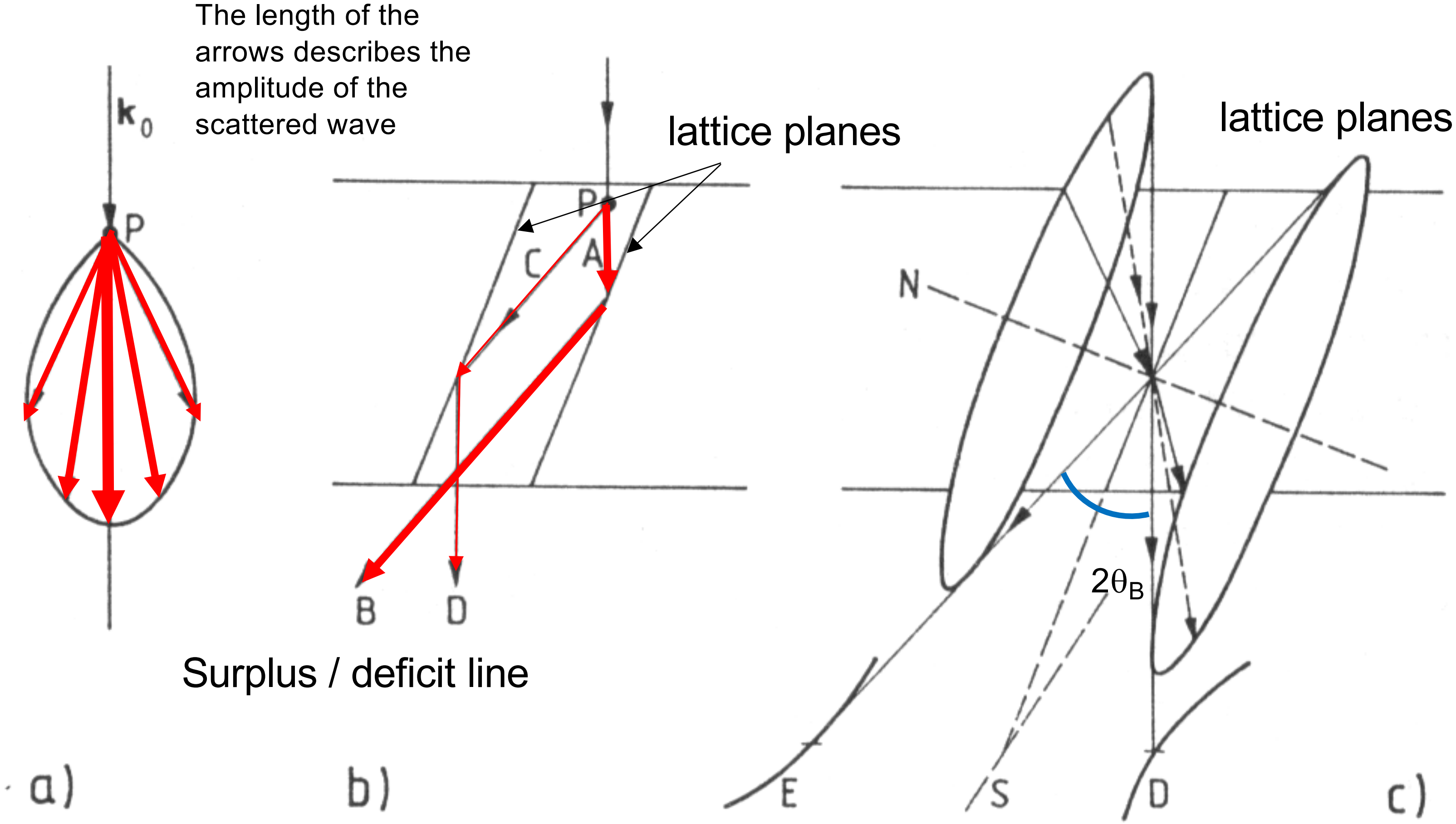

H. Alexander, Physical principles of electron microscopy, Fig. 44

Small Bragg angles → Kikuchi lines are good approximations of straight lines

4.6 Diffraction patterns / Convergent electron diffraction

Two-stage formation mechanism

- Inelastic scattering process with low energy loss
  → *Expansion of the electron beam*

- Some of the scattered electrons fulfill the Bragg condition (two directions possible). The intensity of the Bragg-diffracted electrons is different, i.e. dependent on the angle to the direction of the incident electron wave

- In 3 dimensions: Bragg-diffracted electrons on conical surfaces that intersect the diffraction plane in hyperbolas (approximate straight lines due to small Bragg angles)

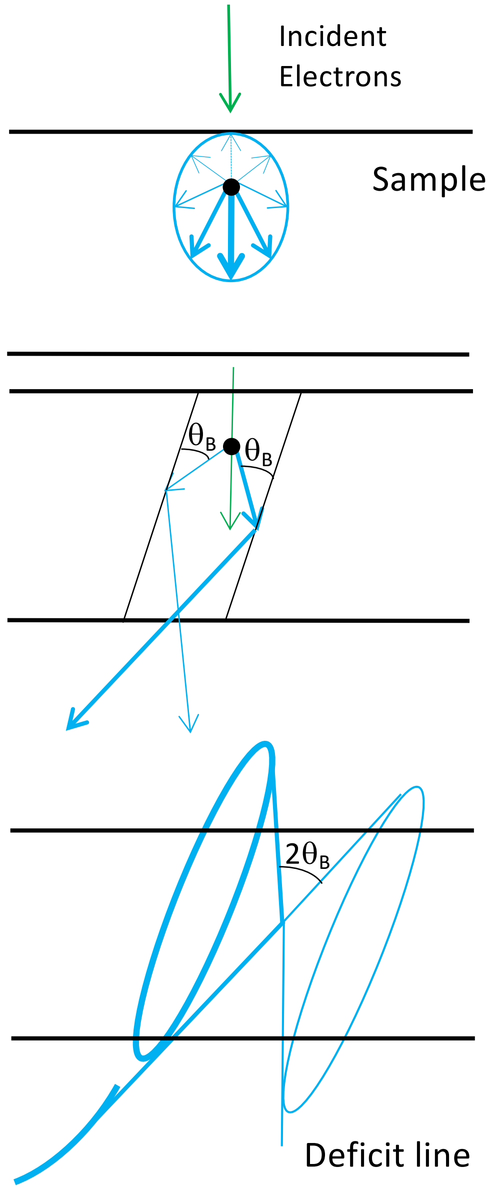

Small Bragg angles → Kikuchi lines are good approximations of straight lines

Laboratory for Electron Microscopy

Kikuchi lines: "Map of the crystal"

Kikuchi lines:

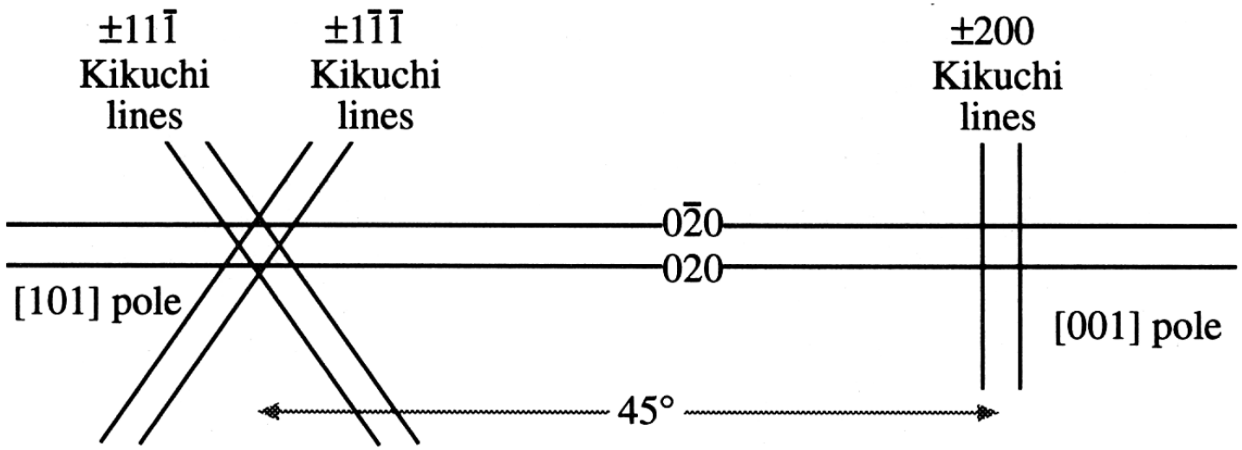

Respective elementary cell projection:

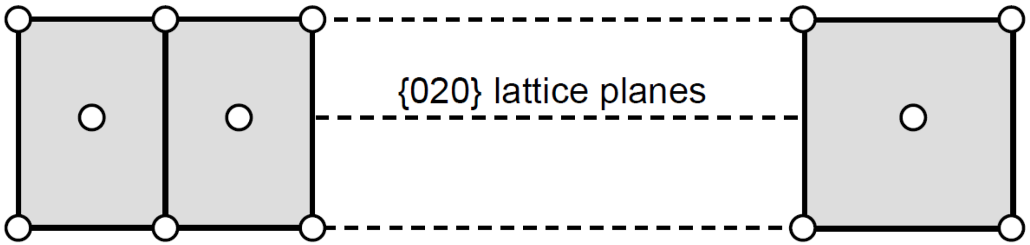

Carter, Williams, Transmission Electron microscopy

Kikuchi lines are very useful for practical work on the TEM:

- Tilting in Bragg condition (two-beam case) for selected reflections.
- Finding low-indexed zone axes and tilting from one zone axis to the other.
- Determination of the excitation error under two-beam conditions.

Laboratory for Electron Microscopy

Kikuchi lines: Determination of the excitation error under two-beam conditions

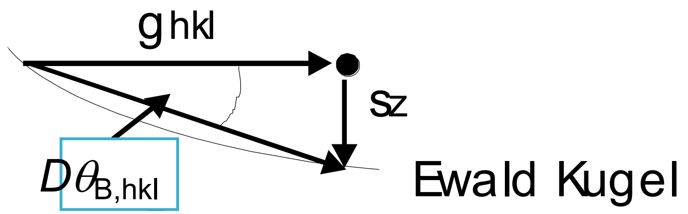

Kikuchi lines are "firmly connected to the grid"
→ Movement when the sample is tilted

Distance between Kikuchi lines leading to a Bragg Reflex g_{hkl} corresponds exactly to $2\theta_{B,hkl}$

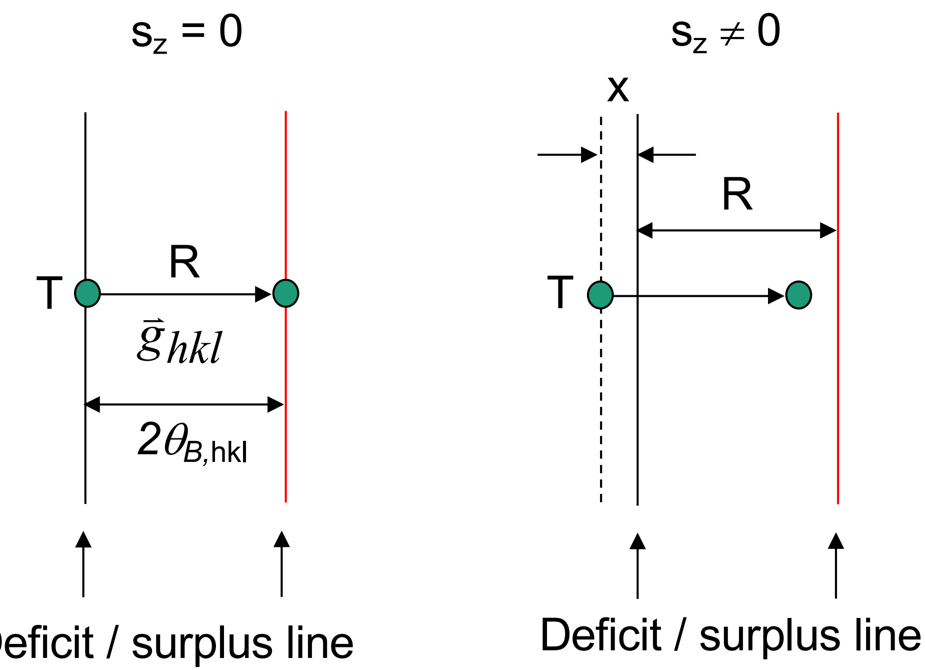

$$s_z \approx |\vec{g}|\Delta\theta_{B,hkl}$$

Measurement of x, R in the diffraction pattern

$$\frac{\Delta\theta_{B,hkl}}{2\theta_B} = \frac{x}{R}$$

Laboratory for Electron Microscopy

Conventional diffraction: single-crystal diffraction patterns

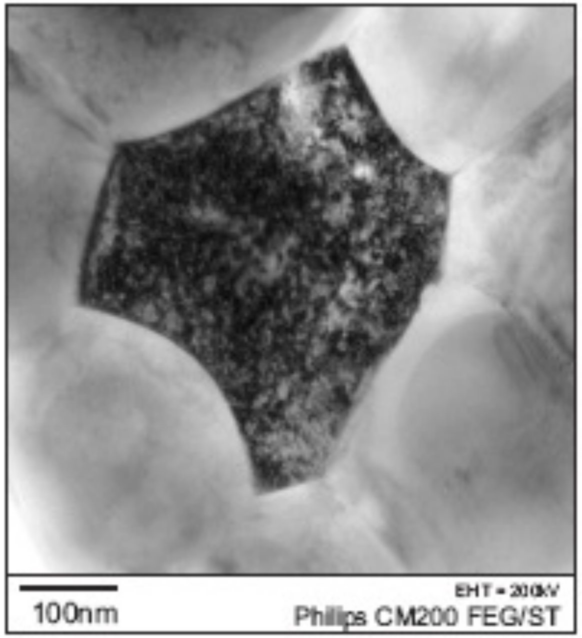

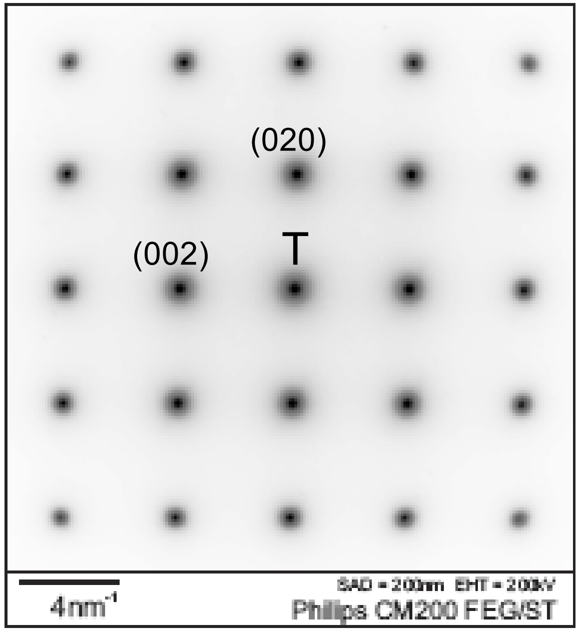

Intensity of the diffraction image inverted for better visibility of the Bragg reflexes

Diploma thesis L. Dieterle, LEM 2006

Determination of the irradiation direction [UVW] (zone axis):
The following applies to all reflexes (hkl) in the diffraction pattern:

$$hU + kV + lW = 0$$

4.6 Diffraction patterns / Convergent electron diffraction

Conventional diffraction: Differentiation of different crystal structures and Crystal structure determination

[100] Zone axis

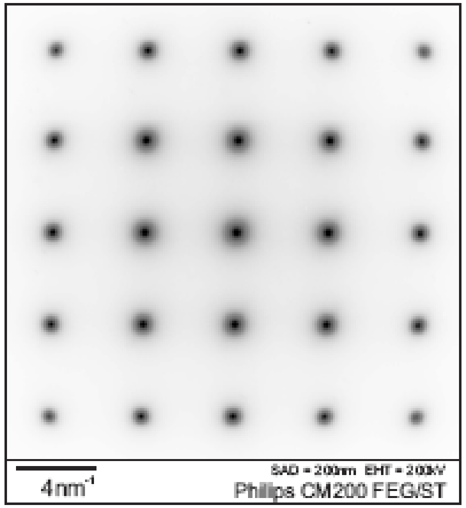

Experimental diffraction image

[100] Zone axis

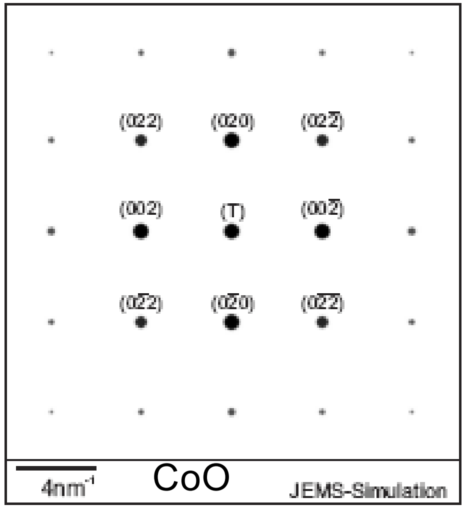

Simulation

[100] Zone axis

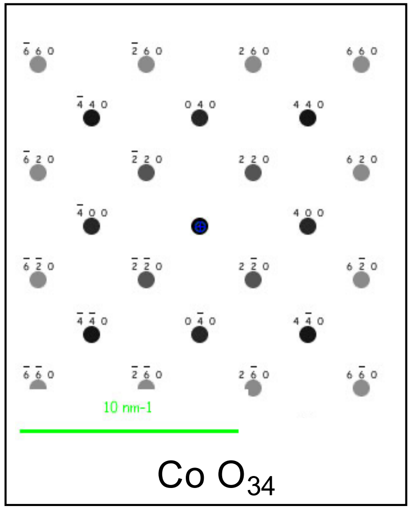

Simulation

Differentiation between different crystal structures Example: Differentiation between CoO and Co O_{34} in [100] Zone axis

Identification of crystal structures by *comparison of experimental and simulated diffraction images* ***along several directions of incidence***

4.6 Diffraction patterns / Convergent electron diffraction

Laboratory for Electron Microscopy

Procedure:

- Measuring the distances and angles in the diffraction pattern
- Calculation of the plane distances
- Simulation of diffraction images of possible crystal structures
  e.g. JEMS from P. Stadelmann http://www.jems-saas.ch/
- Comparison with the simulation

Results of the evaluation:

- Indexing the diffraction images
- Determination of the zone axis
- Calculation of the lattice constant
- Distinction between different phases
- Detection of orientation relationships, e.g. between matrix and precipitate

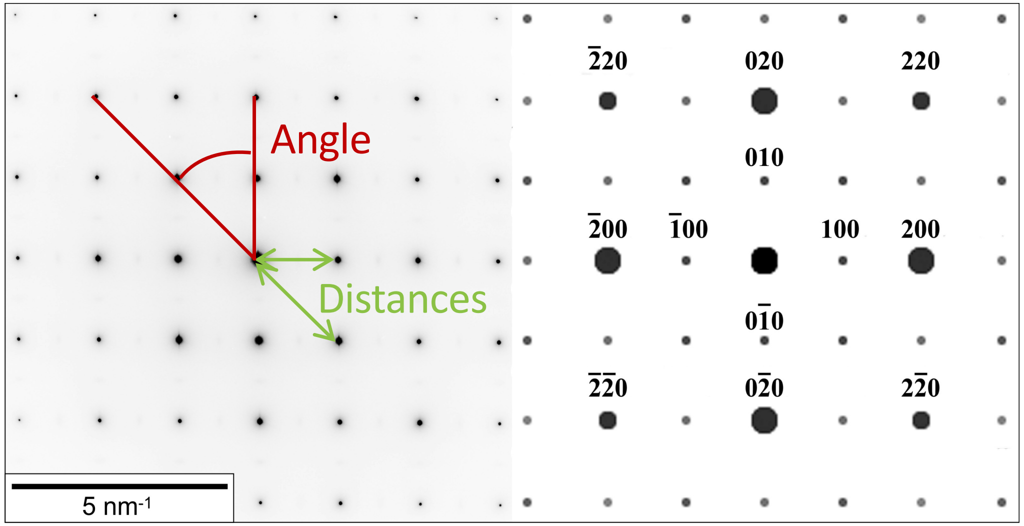

Diffraction image and simulation of $(BaSr)(FeCo)O_3$ cubic, oriented in [100] zone axis

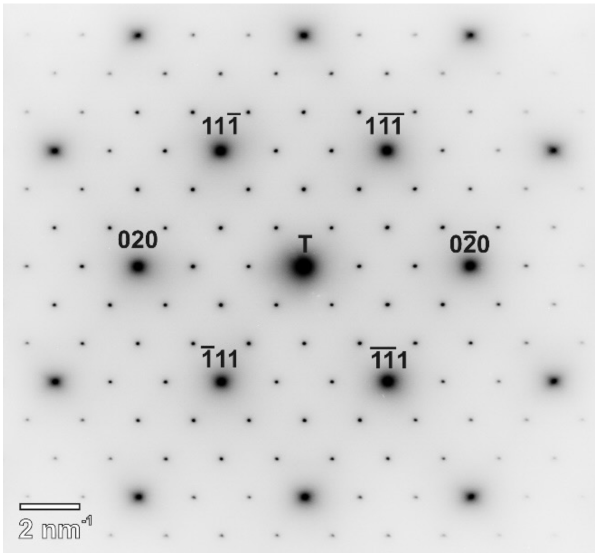

Here: inverted contrast of the diffraction images

Inconel Ni-based super-alloy (face-centered cubic) in [101] zone axis with Reflections of a coherent carbide precipitates

Determination of crystal structures using diffraction images

- Acquisition of several diffraction images along low-index directions such as [100], [110], [111] etc. (zone axis diffraction images)
- Length measurement of $g_{hkl} \rightarrow d_{hkl} = 1/g_{hkl}$
- Identification of kinematically forbidden reflections in thin sample areas as a feature of the crystal structure
- Reflection intensity $I \propto F_S^2$ if conditions for kinematic diffraction are fulfilled
- Symmetry of the reflex arrangement $\rightarrow$ Symmetry of the crystal structure
- No direct calculation of atom positions from diffraction image: "phase problem"
- Comparison of experimental and simulated diffraction images on the basis of possible (guessed) crystal structures (crystal structure data from databases https://icsd.fiz-karlsruhe.de)
- Calculation of diffraction images, e.g. with the program jems by P. Stadelmann (http://www.jems-saas.ch/ free of charge for students)
- **Caution**: dynamic excitation (multiple scattering) of kinematically extinguished reflexes in thicker samples and not necessarily an indication of superstructure
  $\rightarrow$ Record diffraction images in the thinnest possible sample areas

Summary

Laboratory for Electron Microscopy

- Contrasts in crystalline samples are created by lattice defects that disrupt the ordered lattice structure of materials. Classification: Point defects, line-like defects, two-dimensional defects, three-dimensional defects.
- To calculate the scattering amplitude: Let's replace all vectors $\overrightarrow{r_{pi}}$ with $\overrightarrow{r_{pi}} + \vec{R}$ and introduce a displacement vector $\vec{R}$. Here $\vec{R}$, is **much, much smaller** than the lattice plane spacing. $\vec{R}$ indicates the displacement of an atom from its regular lattice position and only affects the lattice amplitude (the structure factor F_s remains unaffected to a good approximation).
- Structure amplitude with displacement vector $\vec{R}$: $\mathrm{F} = F_S \int_0^t \exp(2\pi i[zs_z + \vec{R}\,\vec{g}_{hkl}])dz$
- Special case: If the reciprocal lattice vector $\vec{g}_{hkl}$ is perpendicular to $\vec{R}$ then $\vec{g}_{hkl} \perp \vec{R}$. In this case $\vec{g}_{hkl} \cdot \vec{R} = 0$ and the defect shows no contrast. This special case is used to determine the displacement vector $\vec{R}$**. Two excitation conditions with different reciprocal lattice vectors** are found where $\vec{g}_{hkl} \cdot \vec{R} = 0$. The cross product results in $\vec{R} = \vec{g}_{h_1k_1l_1} \times \vec{g}_{h_2k_2l_2}$.
- Stacking faults are two-dimensional planar defects that occur in crystalline materials and disrupt the stacking sequence (ABCABC) of the most densely packed planes (ABCBABC). The beginning and end of a stacking fault are characterized by partial dislocations.
- Stacking fault contrast is caused by a disturbance of the previously constructively interfering waves. At the location of the stacking fault, the waves are no longer in phase, which causes a reduction in intensity in the bright field image. Stacking faults lying obliquely in the sample generate an oscillating fringe contrast that changes depending on the excitation condition and the imaging condition (HF/DF). These systematic changes are used for stacking fault characterization.
- Dislocations are the carriers of plastic deformation. By displacing the upper half of a crystal relative to the lower half of a crystal by a displacement vector (Burgers vector) $\vec{b}$, a dividing line is created, which is called a dislocation. The Burgers vector has a length and a direction that depends on the crystal structure and the direction of the acting force. Different types of dislocations are characterized by the angle between the Burgers vector $\vec{b}$ and the dislocation line $\vec{u}$. Borderline cases are the screw dislocation ($\vec{b}$ II $\vec{u}$) and the step dislocation ($\vec{b} \perp \vec{u}$).
- The dislocation is described by an extra half-plane in the lattice. The lattice planes bend at the dislocation core (the end of the half plane). The Bragg condition can be fulfilled locally at the bent lattice planes and contrast is created in the image. If **two excitation conditions are** found $\vec{g}_{hkl} \cdot \vec{b} = 0$ and the dislocation thus becomes "invisible", the Burgers vector $\vec{b}$ of the dislocation can be determined via the cross product $\vec{g}_{h_1k_1l_1} \times \vec{g}_{h_2k_2l_2} = \vec{b}$.
- Simulation of dislocation contrasts via column approximation. The "fine structure" of dislocation contrasts is simulated here. It becomes clear that the dislocation contrast depends on the position of the dislocation in the sample depth and on the set excitation error s_z . The larger s_z , the clearer the dislocation contrast.
- **Grain boundaries** are surface-like defects in polycrystalline samples and separate differently oriented monocrystalline areas (grains). Due to the different orientations of the grains, different excitation conditions are fulfilled, which lead to different intensities in the image in an RF or DF image.